Science
AAAS

Supplementary Materials for

Droplet-based forward genetic screening of astrocyte–microglia cross-talk

Michael A. Wheeler *et al*.

Corresponding author: Francisco J. Quintana, fquintana@bwh.harvard.edu

Science **379**, 1023 (2023)
DOI: 10.1126/science.abq4822

The PDF file includes:

Other Supplementary Material for this manuscript includes the following:

Materials and Methods

Mice

Adult male and female mice, and postnatal pups were used on a C57Bl/6J background (#000664, The Jackson Laboratory). Postnatal pups were used from the NF-κB reporter strain FVB.Cg-Tg(HIV-EGFP,luc)8Tsb/J (*26*) (The Jackson Laboratory, #027529) at P0-P3. *Areg-/-* mice were on a C57Bl/6 background and have been previously described (*38*). *Areg*$^{tm2c(EUCOMM)Hmgu}$ (*Areg*$^{f/f}$ mice) (*62*) were crossed to *Cd4::Cre* mice (*68*) to generate *Cd4*^{Areg} conditional KO mice. *Aldh1l1-cre/ERT2* mice (*69*) (The Jackson Laboratory, #029655) were bred to B6.Cg-Gt(ROSA)26Sortm9(CAG-tdTomato)Hze/J mice (*70*) (The Jackson Laboratory, #007909) to generate *Aldh1l1*(*CreERT2/+*)*;TdTomato*(*f/+*) (*TdTomato*^{Aldh1l1}) mice. B6.Cg-Tg(Gfap-cre)73.12Mvs/J mice (*71*) (The Jackson Laboratory, #012886) mice were crossed with *Il33*(*f/f*) mice (*72*) to generate *Gfap*(*Cre/+*)*;Il33*(*f/f*) mice. B6.129P2(C)-Cx3cr1tm2.1(cre/ERT2)Jung/J mice (*73*) (The Jackson Laboratory, #020940) were bred to *Il1rl1*(*f/f*) mice (*72*) to generate *Cx3cr1*(*CreERT2/+*);*Il1rl1*(*f/f*) mice. Both conditional knockout strains were maintained on a C57Bl/6J background for >10 generations, as described (*48*). Conditional deletion of *Il1rl1* or expression of TdTomato was induced at 4-6 weeks of age with 225 mg/kg tamoxifen (Sigma-Aldrich, #T5648), diluted in corn oil (Sigma-Aldrich, #C8267); EAE was induced 4 weeks later. Mice were kept in a pathogen-free facility at the Hale Building for Transformative Medicine at Brigham and Women's Hospital in accordance with the IACUC guidelines. 8–12-week-old mice were used for stereotactic injection and EAE induction. Pups were sacrificed between P0-P3 for harvesting and culturing astrocytes. All procedures were reviewed and approved under the IACUC guidelines at Brigham and Women's Hospital.

Primary bone marrow-derived macrophage cultures

Adult mice were euthanized by rapid cervical dislocation and their legs were aseptically dissected and collected in 50ml Falcon tubes (Thermo Fisher Scientific, #1443222) containing 10 ml ice cold Dulbecco's Phosphate-buffered Saline (DPBS) (Thermo Fisher Scientific, #14190250). Under sterile conditions, skin and muscle were removed from the bone using microdissecting tools and the femur was separated from the tibia. The bones were washed in a petri dish containing 70% ethanol (EtOH) for 3 seconds, dried on a gauze strip and washed in sterile DPBS. The bone epiphysis was cut on both sides and the bone marrow was flushed out with DPBS into a petri dish using a 10ml syringe (BD, #148232A) and a 25-gauge needle (BD, #305122). The bone marrow of 2 bones was collected in a 15 ml Falcon tube (Thermo Fisher Scientific, #352196) and triturated by pipetting 10 times up and down with a 10 ml serological pipette (Corning, #357551). After obtaining a homogenous suspension, the bone marrow was centrifuged for 10 minutes at 400 g and 4°C. Erythrocyte lysis was performed by resuspension of the pellet in ammonium-chloride-potassium (ACK) lysis buffer (Life Technology, #A1049201) and subsequent incubation for 2 minutes at room temperature (RT). To stop the reaction, 9 ml complete medium was added, and the bone marrow was centrifuged for 10 minutes at 400g and 4°C. The pellet was resuspended, and cells were filtered through a 100 µm cell strainer (Fisher Scientific, #22363548) into a fresh 15 ml Falcon tube. Cells were counted using a hemocytometer (Fisher Scientific, #22600100) and resuspended at $10x10^6$ cells/ml in DMEM/F12+GlutaMax (Thermo Fisher Scientific, #10565018) 20% (v/v) FCS (Thermo Fisher Scientific, #10438026) and 1% (v/v) penicillin/streptomycin (PS) (Life Technology, # 15140122), supplemented with 13% (v/v) L929 conditioned medium for BMDMs. Cells were seeded into a 10-cm tissue culture dish (Fisher Scientific, #08772E) and incubated at 37°C 5% CO_2. Additional medium supplemented with L929 conditioned medium was

added after 4 days and fully changed after 6 days of culture. After 10 days, medium was changed to DMEM 20% FCS without growth factors. Cells reached confluency after 10-14 days and were detached by 10 minutes incubation in TrypLE (Thermo Fisher Scientific, #12604021) at 37°C.

Primary astrocyte and microglial cultures from neonatal mice

Procedures were performed as described previously (*74*). Brains of mice aged P0-P3 were dissected into PBS on ice. Cortices were discarded and the brain parenchyma were pooled, centrifuged at 500g for 10 minutes at 4C and resuspended in 0.25% Trypsin-EDTA (Thermo Fisher Scientific, #25200-072) at 37C for 10 minutes. Trypsin was neutralized by adding DMEM/F12+GlutaMAX (Thermo Fisher Scientific, #10565018) supplemented with 10% FBS (Thermo Fisher Scientific, #10438026) and 1% penicillin/streptomycin (Thermo Fisher Scientific, #15140148), and cells were passed through a 70 μm cell strainer. Cells were centrifuged at 500g for 10 minutes at 4C, resuspended in DMEM/F12+GlutaMAX with 10% FBS/1% penicillin/streptomycin and cultured in T-75 flasks (Falcon, #353136) at 37C in a humidified incubator with 5% CO2, for 7-10 days until confluency was reached. Astrocytes were shaken for 30 minutes at 180 rpm, the supernatant was collected for microglia and the media was changed, then astrocytes were shaken for at least 2 hours at 220 rpm and the supernatant was aspirated and the media was changed again. Medium was replaced every 2–3 days. Compound treatment was performed for 2 hours with compounds diluted in DMEM/F12+GlutaMAX (Life Technologies, #10565042) that was supplemented with 10% FBS (Life Technologies, #10438026) and 1% penicillin/streptomycin (Life Technologies, #15140122). For serum free condition, astrocytes was cultured in N1 DMEM/F12 media as described previously (*74*). Compounds used in these studies are: 0.01 pg/mL - 1 μg/mL IL-1β (R&D Systems, #401-ML-005, 100 μg/mL stock in PBS), 2

μg/mL puromycin (Invivogen, #ant-pr-1), 0.01 pg/mL - 1 μg/mL TNFα (R&D Systems, #410-MT-010, 100 μg/mL stock in PBS), 100 ng/mL IL-6 (R&D Systems, #406-ML-005), 200 ng/mL GM-CSF (PeproTech, #315-03), 100 ng/mL LPS-EB (Invivogen, #tlrl-3pelps), 100 ng/mL recombinant mouse IL-33 peptide (R&D Systems, #3626-ML-010), 10 ng/mL AREG (R&D Systems, #989-AR-100, 100 μg/mL stock in PBS). For analysis of cell activation in droplets, compounds were diluted to 2X of their intended working concentrations and co-flowed with cell suspensions for droplet encapsulation. For pre-stimulation experiments, astrocytes were pre-treated with 0.1pg/mL IL-1β/TNFα for 24-hours and subsequently stimulated with the indicated dose of GM-CSF or IL-6 for 24-hours.

Primary microglia culture from adult mice

C57BL/6J mice at least 2 months of age were used. Prior to dissection, one to three mice were anesthetized by isoflurane. Brains were aseptically dissected into 10 ml of enzyme digestion solution consisting of 75 μL Papain suspension (Worthington, #LS003126) diluted in enzyme stock solution (ESS) and equilibrated to 37°C. ESS consisted of 10 ml 10X EBSS (Sigma-Aldrich, #E7510), 2.4 ml 30% D(+)-Glucose (Sigma-Aldrich, #G8769), 5.2 ml 1 M NaHCO3 (VWR, #AAJ62495-AP), 200 μL 500 mM EDTA (Thermo Fisher Scientific, #155750 20), and 168.2 ml ddH2O, filter-sterilized through a 0.22 μm filter. Samples were shaken at 80rpm for 30-40 minutes at 37°C. Enzymatic digestion was stopped by adding 1 ml of 10X Hi-Ovomucoid inhibitor solution and 20 μL 0.4% DNase (Worthington, #LS002007) diluted in 10 ml inhibitor stock solution (ISS). 10X Hi-Ovomucoid inhibitor stock solution contained 300 mg BSA (Sigma-Aldrich, #A8806), 300 mg Ovomucoid Trypsin Inhibitor (Worthington, #LS003086) diluted in 10 ml DPBS and filter sterilized using at 0.22 μm filter. ISS contained 50 ml 10X EBSS (Sigma-Aldrich, #E7510), 6 ml

30% D(+)-Glucose (Sigma-Aldrich, #G8769), 13 ml 1 M NaHCO3 (VWR, #AAJ62495-AP) diluted in 170.4 ml ddH2O and filter-sterilized through a 0.22 μm filter. Tissue was mechanically dissociated using a 5 ml serological pipette and filtered through at 70 μm cell strainer (Fisher Scientific, #22363548) into a fresh 50 ml conical. The mixed suspension was centrifuged at 500g for 5 minutes and resuspended in 10 ml of 30% (v/v) Percoll solution (9 ml Percoll (GE Healthcare Biosciences, #17-544501), 3 ml 10X PBS, 18 ml ddH2O). Percoll suspension was centrifuged at 500g for 25 minutes with no brakes. Supernatant was discarded and the cell pellet was washed with DPBS, centrifuged at 500g for 5 minutes and resuspended in 20 ml prewarmed DMEM/F12 (Gibco, 31331-093) including 10% (v/v) FCS, 1% (v/v) PS (Life Technology, # 15140122), and 13% (v/v) L292 conditioned medium and seeded into an uncoated T75 cell culture flask (Sarstedt, # 831813002). The medium was changed twice a week until the cells reached 90% confluency (12-16 days). To separate the mixed glia culture containing both astrocytes and microglia in an approximatively 2:1 ratio, cells were detached by using 10 ml prewarmed Trypsin-EDTA 0.05% (Thermo Fisher Scientific, #25200-072). After 10-15 minutes incubation in Trypsin-EDTA at 37°C, cells were collected through a 70 μm cell strainer into a 15 ml Falcon tube (Thermo Fisher Scientific, #352196) and the reaction was stopped by adding 5 ml pure FCS. The single cell suspension containing both microglia and astrocytes was centrifuged at 300g at 4°C for 10 minutes. After washing the cells, the pellet was resuspended in 5 ml sterile DPBS and the cells were counted. $CD11B^+$ microglia and $CD11B^-$ astrocytes were separated by using magnetic microbeads attached to an anti-mouse CD11B antibody (Miltenyi Biotec, #130049601) according to the manufacturer's protocol. Following the MACS separation, cells were centrifuged at 300g at 4°C for 5 minutes and resuspended in 5 ml sterile DPBS.

Immunostaining of mouse CNS tissue

Mice were intracardially perfused with ice cold 1X PBS and a 0.5-cm section of the superior spinal column was excised from the mouse then post-fixed in 4% PFA overnight at 4ºC. Following fixation, the vertebral column was de-calcified with 20% EDTA (pH=7.4) for one week at 4ºC with inversion, then the tissue was dehydrated with 30% sucrose for one week at 4ºC. Spinal cords were frozen in OCT (Sakura, #4583) and 20 µm sections were prepared by cryostat on SuperFrost Plus Gold slides (Fisher Scientific, #15-188-48). Sections were permeabilized with 1X permeabilization buffer (BD Biosciences, #554723) for 10 minutes at RT, then blocked using serum-free protein block (Agilent, #X0909) for 10 minutes at RT. Sections were then incubated with primary antibodies diluted in 1X permeabilization buffer overnight at 4ºC. Following primary antibody incubation, sections were washed 3X with 1X permeabilization buffer and incubated with secondary or conjugated antibodies diluted in 1X permeabilization buffer for 1 hour at RT. After secondary and conjugated antibody incubation, sections were stained with 1µg/ml DAPI (Sigma-Aldrich, #D9542) diluted in 1X permeabilization buffer for 5 minutes at RT, then washed 3X with 1X permeabilization buffer and mounted with ProLong Gold Antifade Mountant (Fisher Scientific, #P36930). Primary antibodies used in this study were: goat anti-Amphiregulin (R&D Systems, 1:40, #AF262), rabbit anti-TMEM119 (Abcam, 1:100, #ab209064), mouse anti-GFAP (Millipore, 1:500, #MAB360), chicken anti-GFAP (Abcam, 1:200, #ab4674), rat anti-P2RY12 (Biolegend, 1:100, #848002), rabbit anti-PNOC (Thermo Fisher, 1:500, #PA3204), goat anti-NRTN (R&D Systems, 15µg/mL, #AF477), rabbit anti-ST2 (Abcam, 1:100, #ab25877), and goat anti-IL-33 (R&D Systems, 1:40, #AF3626). Secondary antibodies used in this study were: donkey anti-goat IgG Alexa Fluor 488 (Jackson Immunoresearch, #705-545-003), donkey anti-rabbit IgG (H+L) Highly Cross-Adsorbed, Alexa Fluor 568 (Life Technologies, #A10042), Rhodamine Red-X-

AffiniPure Fab Fragment donkey anti-rabbit IgG (H+L) (Jackson Immunoresearch, #711-297-003), Alexa Fluor 647 AffiniPure Fab Fragment donkey anti-rabbit IgG (H+L) (Jackson Immunoresearch, #711-606-152), donkey anti-goat IgG (H+L) Cross-Adsorbed Secondary Antibody, Alexa Fluor 647 (Fisher Scientific, #A-21447), donkey anti-goat IgG (H+L) Cross-Adsorbed Secondary Antibody, Alexa Fluor 555 (Fisher Scientific, #A-21432), and Alexa Fluor 647 AffiniPure donkey anti-rat IgG (H+L) (Jackson Immunoresearch, #712-605-153) all at 1:1000 working dilution. The conjugated antibody used in this study was mouse anti-GFAP Alexa Fluor 488 (GA5) (Fisher Scientific, 1:100, #53-9892-82). Iterative labeling using rabbit primary antibodies was accomplished by incubating with a single primary antibody on Day 1, staining with the anti-rabbit Fab 568 fragment on Day 2, washing 6X with 1X permeabilization buffer, followed by incubation with primary and secondary antibodies as described above. Sections were imaged and tile scan images were stitched on an LSM-880-AiryScan confocal microscope using the ZEN Black software (Zeiss), and image analysis was performed with FIJI version of ImageJ (NIH).

Microfluidic device fabrication

Master molds for microfluidic device fabrication were fabricated at the Harvard Medical School Microfluidics/Microfabrication Core Facility using common photolithography techniques. Briefly, silicon wafers (University Wafer) were spin-coated with SU-8 photoresist (Kayaku Advanced Materials), patterned with a photomask using ultraviolet light, and baked following the manufacturer's instructions. PDMS devices were fabricated from master molds as follows: Curing agent and PDMS prepolymer (Momentive, #RTV615) were mixed 1:10 and degassed in a vacuum chamber. The PDMS mixture was poured onto the master mold, further degassed, and baked at 65°C for 4 hours. The PDMS replica was punched with a 0.75 mm biopsy punch (Harris Uni-Core)

and bonded to a glass slide (75 x 50 x 1.0 mm, Fisher Scientific, #12-550C) using an oxygen plasma bonder (Technics Plasma Etcher 500-II). The device was placed on a hot plate at 150°C for 10 minutes and baked at 65°C for 4 hours. Finally, channels were rendered hydrophobic by treatment with Aquapel (Aquapel Glass Treatment) for 5 min.

Microfluidic cell encapsulation

For microfluidic cell encapsulation, cells were detached via a 10-minute incubation in TrypLE at 37°C. Cells were washed once and stained with CellTrace Far Red Cell Proliferation Kit (Thermo Fisher Scientific, #C34564) at 1 µM or CellTrace Calcein Red-Orange, AM (Thermo Fisher Scientific, #C34851) at 2 µM for 25 minutes at 37°C. Cells were washed, counted and resuspended at the required density based on the anticipated droplet size in DMEM/F12 without phenol red (Thermo Fisher Scientific, #21041025) + 10% (v/v) FCS and 18-20% (v/v) Opti-prep (Sigma-Aldrich, #D1556-250ML). For optimal droplet detection, Cy5-alkyne (Sigma-Aldrich, #777358) was added with a final concentration of 100 nM to the cell population stained with CellTrace Far Red Cell Proliferation Kit. The cell mixtures were loaded into a 3 ml syringe (BD Biosciences, #309657) with a 27-gauge needle (BD Biosciences. #305109) and connected to the microfluidic device using PTFE tubing (Scientific Commodities, #BB31695-PE/2). For co-encapsulation and in-drop-stimulation experiments, the cell suspensions were injected into the microfluidic device by using a syringe pump at a flow rate of 600 µl/hour. Drops were generated by flow focusing of the resulting stream with QX200 droplet generation oil for EvaGreen (BioRad, #1864006) at a flowrate of 3000 µl/hour. The resulting emulsion was collected in 3 ml syringes (BD, #148232A) for reinjection or in a 15 ml Falcon tube (Thermo Fisher Scientific, #352196) for cell viability assessment. The emulsion was incubated at 37°C 5% CO_2 for 10-72 hours.

Reinjection and sorting of droplets

After incubation of cell-containing droplets, the emulsion was reinjected onto a custom droplet-sorter as described in (*25*). In brief, the emulsion containing monodisperse drops was re-injected into a microfluidic device by using a syringe pump (Harvard Apparatus, milliliter OEM syringe pump) at a flow rate of 200 µl/hour. Drops were spaced by injection of 3M Novec 7500 Engineered Fluid (HFE; 3M, #Novec 7500) at a flow rate of 300 µl/hour. Electrode and moat channels were loaded with 2M NaCl solution. Detection of droplet fluorescence was performed using a custom in-house 3-color droplet cytometer. Three lasers (473 nm, 532 nm, 638 nm) are aligned via dichroic mirrors and focused on the microfluidic device mounted on a microscope (Motic AE31). A custom LabView (National Instruments) program was used to run a field programmable gate array (FPGA; National Instruments) to control photomultiplier tubes (PMT) (PMM01/PMM02, Thorlabs) for fluorescence detection. Based on a pre-determined fluorescence-threshold, positive drops were sorted, using a concentric electrode design, into a separate output channel by actuating electric pulses via a high-voltage amplifier (Trek). Negative and positive populations were collected in 15 ml Falcon tubes (Thermo Fisher Scientific, #352196) and the resulting oil-phase was overlaid with 200 µl DPBS (Thermo Fisher Scientific, #14190250). For optimal droplet recovery, the emulsion was frozen at -80°C. Peak droplet fluorescence values were recorded, exported, and analyzed in FlowJo.

Droplet stability assessment

To assess droplet stability, primary astrocytes were encapsulated at 1 cell in every 10 drops as described above. The cells were resuspended and encapsulated in the following combinations

of medium ± surfactant, 10% (v/v) FCS (Thermo Fisher Scientific, #10438026) and 18% (v/v) Opti-prep (Sigma-Aldrich, #D1556-250ML): (i) DMEM/F12 with phenol red (Thermo Fisher Scientific, #11320033), (ii) DMEM/F12 without phenol red (Thermo Fisher Scientific, #21041025), (iii) DMEM/F12 without phenol red + 0.1% (w/v) bovine serum albumin (Sigma-Aldrich, #A32944), and (iv) DMEM/F12 without phenol red + 0.1% (v/v) + Pluronic F-68 (Thermo Fisher Scientific, #24040032). Droplets were collected in 15 ml Falcon tubes (Thermo Fisher Scientific, #14190250) and droplet stability was assessed by imaging on a Leica DMi8 Inverted Microscope as the number of coalesced droplets after one day of incubation at 37°C 5% CO2. To assess the transport of soluble protein between drops, 1 μM Bovine Serum Albumin (BSA) conjugated with tetramethylrhodamine (Thermo Fisher Scientific, #A23016) or 1 μM BSA conjugated with Alexa Fluor 647 (Thermo Fisher Scientific, #A34785) were separately encapsulated in 65-micron droplets with DMEM/F12 without phenol red (Thermo Fisher Scientific, #21041025) + 0.1% (v/v) Pluronic F-68 using droplet generation oil for EvaGreen (BioRad, #1864006). Drops were mixed, incubated for 24 hours, and imaged using an ECHO Revolve Fluorescence Microscope.

Cell recovery and viability assessment

To quantify cell viability cells were stained with CellTrace Calcein Red-Orange (Thermo Fisher Scientific, #C34851) according to the manufacturer's protocol prior to encapsulation. After droplet encapsulation, the oil phase was aspirated and droplets were merged and broken using 20% (v/v) 1H,1H,2H,2H-perfluoro-1-octanol (PFO; Sigma-Aldrich, #370533) in HFE (3M, #Novec 7500) to recover the cells trapped inside droplets. After the PFO break, the aqueous phase was separated by centrifugation at 30g for 30 seconds and transferred into a fresh tube. Cells were

washed and live cells were quantified by FACS on a BD LSRFortessa. To acquire micrographs of cells post-encapsulation, 10 μL of the emulsion was collected in a cell counting chamber slide (Thermo Fisher Scientific, #C10228) and imaged on a Leica DMi8 inverted microscope.

Genome-scale CRISPR/Cas9 library production

Amplification and sequencing of the plasmid library was performed as previously described (*75*). Briefly, a mouse CRISPR/Cas9 pooled lentiviral library consisting of 78,637 gRNAs targeting 19,674 mouse genes (*29*) (lentiCRISPRv2, Brie, Addgene #73632, a gift from David Root and John Doench) was obtained and amplified by transformation of STBL4 electrocompetent cells (Thermo Fisher Scientific, #11635018) according to the Broad Institute's Protocol: *"Amplification of pDNA libraries"*. After 16-18 hours of growth, pellets were collected and the library purified using an endofree plasmid maxi kit (Qiagen, #12362) according to the manufacturer's protocol with two modifications: a) add P1, P2, P3 directly to the conical and centrifuge to pellet lysed debris before adding to plunger; b) warm elution buffer to 50°C before eluting. Lentivirus production was performed as previously described (*21*). The pooled library was co-transfected with packaging plasmids (psPAX2, Addgene #12260 and pCMV-VSV-G, Addgene #8454) into HEK293T cells using LT-1 transfection reagent (Mirus Cat# MIR2305) following the manufacturer's protocol. psPAX2 was a gift from Didier Trono (Addgene plasmid #12260; http://n2t.net/addgene:12260; RRID:Addgene 12260). pCMV-VSV-G was a gift from Bob Weinberg (Addgene plasmid #8454; http://n2t.net/addgene:8454; RRID:Addgene_8454) (*76*). Library DNA (37 μg), psPAX2 DNA (46 μg) and VSV-G DNA (4.62 μg) was mixed and transfected into HEK293T cells in a T175 flask (Corning, #353112). Six hours after transfection, media was removed and replaced with 40 ml of virus production media (DMEM/F12 (Thermo

Fisher Scientific, #11320033) + 20% (v/v) FCS (Thermo Fisher Scientific, #10438026)). Forty-eight hours after transfection, lentiviral media was harvested and stored in -80C. Cells were transduced at a MOI of 0.4, as described (*75*). In brief, cells were detached by using 10 ml prewarmed Trypsin-EDTA 0.05% (Thermo Fisher Scientific, #25200-072), counted and resuspended at $1.5x10^6$ cells/ml in growth medium supplemented with 16 µg/ml Polybrene (Millipore, #TR1003G) and the respective volume of lentiviral media.

Amplification and analysis of sgRNA sequences from sorted droplets

After droplet encapsulation and sorting, the sgRNA target region was amplified and sequenced following the Broad Institute's protocol: *"PCR of sgRNAs from gDNA for Illumina Sequencing".* Sorted droplets were placed in the -80C for a minimum of 24 hours, thawed at room temperature for 1 hour, and broken by adding 1 ml 20% (v/v) PFO in HFE (3M, #Novec 7500). For optimal phase separation, the emulsion was gently mixed by tapping the tube and subsequently centrifuged at 1000 g for 30 seconds. The aqueous layer containing the sorted cells was aspirated and transferred to a fresh 1.5 ml microcentrifuge tube. Genomic DNA (gDNA) was isolated using a Blood & Tissue DNA isolation kit (Qiagen, #69504) according to the manufacturer's protocol. The genomic DNA was eluted in a final volume of 400 µl and subsequently concentrated to 40 µl by 2.0X AMPure XP bead purification according to the manufacturer's protocol (Beckman Coulter, #A63880). Next, the sgRNA libraries were amplified according to the Broad Institute's Protocol: *"Amplification of pDNA libraries".* In brief, positive samples containing less than 2000 droplets were PCR amplified for 35 cycles, negative samples with more than 2000 droplets were PCR amplified for 28 cycles. A staggered forward primer cocktail, made by combining equimolar concentrations of

P5 0 nt stagger 5’-ATGATACGGCGACCACCGAGATCTACACTCTTTCCCTACACGA CGCTCTTCCGATCTGATGTCCACGAGGTCTCT-3’, P5 1nt stagger 5’-AATGATACGGCGACCACCGAGATCTACACTCTTTCCCTACACGACGCTCTTCCGATC TCGATGTCCACGAGGTCTCT-3’, P5 2 nt stagger 5’-AATGATACGGCGACCACCGAGATCTACACTCTTTCCCTACACGACGCTCTTCCGATC TGCGATGTCCACGAGGTCTCT-3’, P5 3 nt stagger 5’-AATGATACGGCGACCACCGAGATCTACACTCTTTCCCTACACGACGCTCTTCCGATC TAGCGATGTCCACGAGGTCTCT-3’, P5 4 nt stagger 5’-AATGATACGGCGACCACCGAGATCTACACTCTTTCCCTACACGACGCTCTTCCGATC TCAACGATGTCCACGAGGTCTCT-3’, P5 5 nt stagger 5’-AATGATACGGCGACCACCGAGATCTACACTCTTTCCCTACACGACGCTCTTCCGATC TTGCACCGATGTCCACGAGGTCTCT-3’, P5 6 nt stagger 5’-AA TGATACGGCGACCACCGAGATCTACACTCTTTCCCTACACGACGCTCTTCCGATCTA CGCAACGATGTCCACGAGGTCTCT-3’, P5 7 nt stagger 5’-AATGATACGGCGACCACCGAGATCTACACTCTTTCCCTACACGACGCTCTTCCGATC TGAAGACCCGATGTCCACGAGGTCTCT-3’, P5 8 nt stagger 5’-5’-AATGATACGGCGACCACCGAGATCTACACTCTTTCCCTACACGACGCTCTTCCGATC TGAAGACCCTTGTGGAAAGGACGAAACACCG-3’, and a unique P7 primer for use with lentiCRISPRv2:

5’CAAGCAGAAGACGGCATACGAGAT<u>NNNNNNNN</u>GTGACTGGAGTTCAGACGTGTG CTCTTCCGATCTCCAATTCCCACTCCTTTCAAGACCT-3’ were used. Following library amplification, the samples were purified using 2.0X AMPure XP bead purification and eluted in 40 µl H2O. Finally, the sgRNA libraries were sized on an Agilent 2100 Bioanalyzer and their

concentration determined using a KAPA Library Quantification Kit (Kapa Biosystems, #KK4824) according to the manufacturer's protocol. Libraries were sequenced at 1x75bp at the Harvard Biopolymers Facility on a MiSeq Micro or in the Neurotechnology Studio of Brigham and Women's Hospital on a NextSeq550. Raw sequencing reads were trimmed using cutadapt to find sgRNA sequences matching those contained in the genome-wide library (-g ACACCG...GTTTTAG) and counted using MAGeCK (*77*). The non-targeting guides with high fold enrichment in Fig. S5K are control285 and control946 from the Brie library.

Rationale and criteria for selecting positive hits

To filter the hits detected by SPEAC-seq against physiologically relevant processes in microglia, we retained for analysis only SPEAC-seq genes detected in a filtered bulk RNA-seq dataset of primary microglia treated with 100 ng/mL of LPS-EB (Invivogen, #tlrl-3pelps) or vehicle. In addition, we validated this filtered list against four previously published mouse bulk and single-cell RNA-seq studies that analyzed microglia gene expression in vivo in health and disease (*27, 34, 35, 78*).

CRISPR/Cas9 lentivirus production

Lentiviral constructs were generated as previously described (*12, 27, 37*). The backbones used contain derivatives of the previously described reagents lentiCRISPR v2 (a gift from Feng Zhang, Addgene plasmid #52961 (*79*)), and lentiCas9-EGFP (a gift from Phil Sharp and Feng Zhang, Addgene plasmid #63592 (*17*)). *Itgam*-driven lentiviruses have been previously described (*11, 12*). Substitution of sgRNAs was performed through a PCR-based cloning strategy using Phusion Flash HF 2X Master Mix (Thermo Fisher, #F548L). A three-way cloning strategy was

developed to substitute sgRNAs using the following primers: U6-PCR-F 5'-AAAGGCGCGCCGAGGGCCTATTT-3', U6-PCR-R 5'-TTTTTTGGTCTCCCGGTGTTTCGTCCTTTCCAC-3', cr-RNA-R 5'-GTTCCCTGCAGGAAAAAAGCACCGA-3', cr-RNA-F 5'-AAAAAAGGTCTCTACCG(N_{20})GTTTTAGAGCTAGAAATAGCAAGTT-3', where N_{20} marks the sgRNA substitution site. The following sgRNA were designed using a combination of the Broad GPP sgRNA Designer Webtool (SpyoCas9, http://portals.broadinstitute.org/gpp/public/analysis-tools/sgrna-design), Synthego (https://design.synthego.com/#/), and cross-referenced with activity-optimized sequences contained within the Addgene library #1000000096 (a gift from David Sabatini and Eric Lander) (*80*). The sgRNA sequences used are as follows, with the promoter indicated in parentheses: *sgScrmbl* - 5'-GCACTACCAGAGCTAACTCA-3' (*Itgam*, *Gfap*); *sgAreg* 5'-AATGACCCCAGCTCAGGGAA-3' (*Itgam*); *sgFgl1* - 5'-CCAGTTTCTGGATAAAGGAT-3' (*Itgam*); *sgPnoc* - 5'-AGACCTTCTCTTCACACTGG-3' (*Itgam*); *sgNrtn* - 5'-GCTGGGCCTGGGCTACACGT-3' (*Itgam*); *sgEgfr* - 5'-GATGTACAACAACTGTGAAG-3' (*Gfap*); *sgGfra2* - 5'-GGCCAATAAGGAGTGCCAGG-3' (*Gfap*); *sgLag3* - 5'-GCCTGGGAAAGAGCTCCCCG-3' (*Gfap*); and *sgOprl1* 5'-TGAGGATGACATACATGACG-3' (*Gfap*). Amplicons were purified using the QIAquick PCR Purification Kit (Qiagen, #28104) and digested using DpnI (NEB, #R0176S), BsaI-HF (NEB, #R3535/R3733), AscI (for U6 fragment) (NEB, #R0558), or SbfI-HF (for crRNA fragment) (NEB, #R3642). pLenti backbone was cut with AscI/SbfI-HF and purified using the QIAquick PCR purification kit. Ligations into the respective backbone were performed overnight at 16°C using T4 DNA Ligase Kit (NEB, #M0202L). Ligations were transformed into NEB Stable *E. Coli* (NEB, #C3040) at 42°C and the

ligation products were spread onto ampicillin selection plates. After overnight incubation at 37°C, single colonies were picked and DNA was prepared using QIAprep spin miniprep kit (Qiagen, #27104).

To generate barcoded lentiviral vectors, DNA oligonucleotides containing a barcode sequence were annealed into a degenerate dsDNA fragment with overhangs corresponding to 5' BsrGI and 3' EcoRI cut sites, which inserted barcodes immediately 3' of the EGFP translational stop contained in *Gfap*::Cas9-2A-EGFP. Annealing was performed according to a protocol from Addgene by mixing 2 µg of each primer in 50 µL of annealing buffer (10mM Tris pH=7.5, 50 mM NaCl, 1 mM EDTA), heating the tube to 95C in a heat block, then moving the heat block to the bench top until it reached room temperature. The oligonucleotides used for this protocol were: FWD: 5'-GTACAAGTAANNNNNNNNGATGTCCACGAGGTCTCTGCTAGCG-3' and REV: 5'-AATTCGCTAGCAGAGACCTCGTGGACATCNNNNNNNNTTACTT-3' where NNNNNNNN represents the barcode sequence. Barcode sequences (5'->3') used for this study were: *sgScrmbl*: CGTACTAG, *sgEgfr*: CTCTCTAC, *sgGfra2*: CAGAGAGG, *sgLag3*: GCTACGCT, and *sgOprl1*: CGAGGCTG.

Lentiviral plasmids were transfected into HEK293FT cells according to the ViraPower Lentiviral Packaging Mix protocol (Thermo Fisher Scientific, #K497500) and lentiviruses were packaged with pLP1, pLP2, and pseudotyped with pLP/VSVG. Supernatant was aspirated the following day and fresh medium was added. After 2 days of incubation, lentivirus was collected and concentrated using Lenti-X Concentrator (Clontech, #631231) overnight at 4°C followed by centrifugation according to the manufacturer's protocol. Lentiviral pellets were resuspended in 1/500 of the original volume and stored at -80°C.

Intracranial lentivirus injection

C57Bl/6J mice at age 8-12 weeks were anesthetized using 1-3% isoflurane mixed with oxygen. Heads were shaved and cleaned using 70% ethanol and Betadine (Thermo Fisher, #19-027132) followed by a medial incision of the skin to expose the skull. The lateral ventricles were targeted bilaterally using the coordinates: +/- 1.0 (lateral), -0.44 (posterior), -2.2 (ventral) relative to Bregma. Mice were injected with approximately 10^7 total IU of lentivirus delivered by two 10 µL injections using a 25 µL Hamilton syringe (Sigma-Aldrich, #20787) on a stereotaxic alignment system (Kopf, #1900) and the incision was sutured. Mice received 1 mg/kg Buprenorphine-SR via subcutaneous injection and were permitted to recover 7 days in a separate clean cage before induction of EAE. For Perturb-seq experiments, an equimolar cocktail of each barcoded lentivirus was injected +1.25 (lateral), +1.0 (rostral), -3.0 (ventral) relative to Bregma. For in vivo AREG treatment, mice were injected with 100 ng of AREG (R&D Systems, #989-AR-100) in 5 µL PBS or 5 µL of vehicle using the coordinates: +/- 1.0 (lateral), -0.44 (posterior), -2.2 (ventral) relative to Bregma.

EAE induction

EAE was induced with 150 µg of MOG_{35-55} (Genemed Synthesis Inc., #110582) emulsified in freshly prepared complete Freund's adjuvant (Incomplete Freund's Adjuvant (BD Biosciences, #BD263910) mixed with mycobacterium tuberculosis H-37Ra (BD Biosciences, #231141); final concentration 5 mg/ml). All animals received 2 subcutaneous injections of 100 µL each of MOG and a single intraperitoneal injection of 400 ng pertussis toxin (List Biological Laboratories, #180) in 200 µL of PBS. Mice received a second injection of pertussis toxin 48 hours after the initial injection. Mice were monitored and clinical scores were documented daily until the end of the

experiment. Mice were sacrificed at different time points of disease. EAE clinical scores were defined as follows: 0 – no signs, 1 – fully limp tail, 2 – hindlimb weakness, 3 – hindlimb paralysis, 4 – forelimb paralysis, 5 – moribund.

ELISA

Costar 96-well plates (Corning, #3690) were coated with capture antibodies diluted in 1X PBS: anti-mouse TNF-α capture (Invitrogen, #88-7324-88, 1:250), anti-mouse IL-1 beta capture (Invitrogen, #88-7013-88, 1:250), overnight at 4°C. Plates were washed 3 times with 0.05% Tween in 1× PBS (Boston BioProducts, #IBB-171X) and blocked with 1X Elispot diluent (eBioscience, #00-4202-56) for 1h at room temperature. The standard curve was prepared from 1 ng ml^{-1} protein diluted in 1X Elispot diluent. Samples were undiluted. Plates were washed 3 times with 0.05% Tween in 1× PBS and samples and standard curve were added and incubated overnight at 4 °C. The next day, plates were washed 3 times with 0.05% Tween in 1X PBS and incubated with detection antibodies diluted in 1X Elispot diluent: anti-mouse TNF-α detection (Invitrogen, #88-7324-88, 1:250), anti-mouse IL-1 beta detection (Invitrogen, #88-7013-88, 1:250), for 1h at room temperature. Afterwards, plates were washed 3 times with 0.05% Tween in 1× PBS and incubated with Avidin-HRP diluted in 1X Elispot diluent (Invitrogen, #88-7324-88, 1:100) for 1 h at room temperature. Next, plates were washed 6 times with 0.05% Tween in 1X PBS and revealed using 1X TMB Substrate Solution (Invitrogen, #00-4201-56) for 15 minutes at room temperature. The reaction was stopped by KPL TBM Stop Solution (SeraCare, #5150-0021) and plates were read at 450 nm with 560nm reference value on a GloMax Explorer Multimode Microplate Reader (Promega).

Isolation of cells from the adult CNS

Astrocytes were isolated by flow cytometry as described (*11-13, 27, 37, 81*) and by modifying a previously described protocol (*82*). Briefly, mice were perfused with 1X PBS and the CNS was isolated into 10 mL of enzyme digestion solution consisting of 75 µL Papain suspension (Worthington, #LS003126) diluted in enzyme stock solution (ESS) and equilibrated to 37C. ESS consisted of 10 mL 10X EBSS (Sigma-Aldrich, #E7510), 2.4 mL 30% D(+)-Glucose (Sigma-Aldrich, #G8769), 5.2 mL 1M NaHCO3 (VWR, #AAJ62495-AP), 200 µL 500 mM EDTA (Thermo Fisher Scientific, #15575020), and 168.2 mL ddH2O, filter-sterilized through a 0.22 µm filter. Samples were shaken at 80rpm for 30-40 minutes at 37C. Enzymatic digestion was stopped with 1 mL of 10X hi ovomucoid inhibitor solution and 20 µL 0.4% DNase (Worthington, #LS002007) diluted in 10 mL inhibitor stock solution (ISS). 10X hi ovomucoid inhibitor stock solution contained 300 mg BSA (Sigma-Aldrich, #A8806), 300 mg ovomucoid trypsin inhibitor (Worthington, #LS003086) diluted in 10 mL 1X PBS and filter sterilized using at 0.22 µm filter. ISS contained 50 mL 10X EBSS (Sigma-Aldrich, #E7510), 6 mL 30% D(+)-Glucose (Sigma-Aldrich, #G8769), 13 mL 1M NaHCO3 (VWR, #AAJ62495-AP) diluted in 170.4 mL ddH2O and filter-sterilized through a 0.22 µm filter. Tissue was mechanically dissociated using a 5 mL serological pipette and filtered through at 70 µm cell strainer (Fisher Scientific, #22363548) into a fresh 50 mL conical. Tissue was centrifuged at 500g for 5 minutes and resuspended in 10 mL of 30% Percoll solution (9 mL Percoll (GE Healthcare Biosciences, #17-5445-01), 3 mL 10X PBS, 18 mL ddH2O). Percoll suspension was centrifuged at 500g for 25 minutes with no brakes. Supernatant was discarded and the cell pellet was washed 1X with 1X PBS, centrifuged at 500g for 5 minutes and prepared for downstream applications.

10X Genomics scRNA-seq

After Percoll separation described above, 3' CellPlex Kit (10X Genomics, #PN-1000261) was used for multiplexing each biological replicate according to the manufacturer's protocol. After multiplexing, cells were loaded onto a single lane of Chromium Next GEM Chip G (10X Genomics, #PN-2000177) and processed on a Chromium instrument (10X Genomics). Gene expression and multiplex libraries were prepared using the Single Cell 3′ Reagent Kits v3.1 (10X Genomics) according to the manufacturer's protocol. cDNA samples were amplified using the following PCR conditions: 98C (3min); [11-12 cycles of: 98C (15sec), 63C (20sec), 72 C (1min)]; 72C (1min); 4C hold. Following PCR, cDNA samples were purified on a 10X magnetic Separator (#PN-230003) using SPRIselect reagent (Beckman Coulter, #B23317). cDNA was run on a Bioanalyzer High Sensitivity DNA chip (Agilent Technologies, #5067-4626) on a 2100 Bioanalyzer. 10µL of cDNA was used for generating 3' gene expression library and were indexed uniquely using the Dual Index Plate TT Set A (10X Genomics, #PN-3000431). Samples underwent PCR using the following conditions: 98C (45sec); [14 cycles of: 98C (20sec), 54C (30sec), 72C (20sec)]; 72C (1min); 4C hold. For generating cell multiplex libraries, 5µL of cDNA was used and indexed uniquely using the Dual Index Plate NN Set A (10X Genomics, #PN-3000482). Samples underwent PCR using the following conditions: 98C (45sec); [6 cycles of: 98C (20sec), 54C (30sec), 72C (20sec)]; 72C (1min); 4C hold. Libraries were purified using SPRIselect reagent. Samples were then run on a 2100 Bioanalyzer to access library size and were quantified by qPCR using a Library Quantification Kit (Kapa Biosystems, #KK4824). Libraries were pooled and sequenced on a NovaSeq 6000 (28+72 cycles) at an average depth of 380,763 reads/cell, 2,539 genes/cell, and 10,655 UMIs/cell.

Perturb-seq barcode isolation

Whole transcriptome amplified cDNA (WTA product) was PCRed using the following: 1-5µL WTA product, 1 µL of 50 µM EGFP_R cDNA amplification primer (5'-TGCTGGAGTTCGTGACCGCC-3'), 1 µL of 50 µM 10X Genomics cDNA Forward Primer (5'-CTACACGACGCTCTTCCGATCT-3'), 25 µL of NEBNext High-Fidelity 2X PCR Master Mix (NEB, #M0541L) and molecular grade water to fill a 50 µL reaction under the cycling conditions: 98C for 30 sec, 25 cycles of [98C for 20s, 63C for 30s, 72C for 60 sec], 72C for 120 sec, and 4C forever. Samples were then purified using 2.0X Ampure XP magnetic beads (Beckman-Coulter, #A63881) according to the manufacturer's protocol. DNA was resuspended in 15 µL of DNase/RNase-free water. Next, cDNA samples were PCRed using the following conditions: 3 µL purified PCR product from round 1, 25 µL NEBNext High-Fidelity 2X PCR Master Mix, 1 µL 10 µM Chromium i7 Sample Index (10X Genomics, #PN-220103) (5'-AATGATACGGCGACCACCGAGATCTACACTCTTTCCCTACACGACGCTC-3') and 1 µL of 10 µM GFP-5XX-R (5'-CAAGCAGAAGACGGCATACGAGATXXXXXXXXGTGACTGGAGTTCAGACGTGTGCTCTTCCGATCTTGCTGGAGTTCGTGACCGCC-3'). Samples were cycled using the following conditions: 98C for 30 sec and 10 cycles of [98C for 20s, 55C for 20s, 72C for 60s], followed by 72C for 2 minutes, and 4C forever. Following PCR, samples were purified using a 2.0X Ampure XP bead purification and resuspended in 15 µL of H2O. Samples were then quantified on a 2100 Bioanalyzer (Agilent Technologies). Samples were quantified by qPCR prior to deep sequencing using the Kapa Library Quantification Kit (Kapa Biosystems, #KK4824). After sequencing, the barcodes were counted using unique molecular identifiers and associated with cell barcode sequences. Barcodes associated with each perturbation were then quantified for each cell. Cells

were assigned to each perturbation group based on UMI-normalized abundance of each Perturb-seq barcode in each cell.

Flow cytometry

Cells were stained in the dark on ice for 15 minutes with flow cytometry antibodies. Cells were then washed once with 1X PBS and resuspended in 1X PBS for sorting as described previously (*11-13, 27, 37, 81*). Antibodies used in this study were: PE anti-mouse CD45R/B220 (BD Biosciences, #553089, 1:100), PE anti-mouse TER-119 (Biolegend, #116207, 1:100), PE anti-O4 (R&D Systems, #FAB1326P, 1:100), PE anti-CD105 (eBioscience, #12-1051-82, 1:100), PE anti-CD140a (eBioscience, #12-1401-81, 1:100), PE anti-Ly-6G (Biolegend, #127608, 1:100), PerCP anti-Ly-6C (Biolegend, #128028, 1:100), APC anti-CD45 (eBioscience, #17-0451-83, 1:100), APC-Cy7 anti-CD11c (BD Biosciences, #561241, 1:100), and FITC anti-CD11b (eBioscience, #11-0112-85, 1:100). For Perturb-seq experiments, the following antibodies were substituted BV737-CD11b (BD, #612800, 1:100), BV786-Ly6C (BD, #740850, 1:100). All cells were gated on the following parameters: $CD105^{neg}CD140a^{neg}O4^{neg}Ter119^{neg}Ly\text{-}6G^{neg}CD45R^{neg}$. Astrocytes were subsequently gated on: $CD11b^{neg}CD45^{neg}Ly\text{-}6C^{neg}CD11c^{neg}$. Microglia were subsequently gated on: $CD11b^{high}CD45^{low}Ly\text{-}6C^{low}$. Pro-inflammatory monocytes were subsequently gated on: $CD11b^{high}CD45^{high}Ly\text{-}6C^{high}$. Compensation was performed on single-stained samples of cells and an unstained control. Cells were sorted on a FACS Aria IIu (BD Biosciences).

RNA expression analysis of primary mouse astrocytes

Primary astrocytes were lysed in Buffer RLT (Qiagen) and RNA was isolated from cultured

astrocytes using the Qiagen RNeasy Mini kit (Qiagen, #74106). cDNA was transcribed using the High-Capacity cDNA Reverse Transcription Kit (Life Technologies, #4368813). Gene expression was then measured by qPCR using Taqman Fast Universal PCR Master Mix (Life Technologies, #4367846). Taqman probes used in this study are: *Gapdh* (Mm99999915_g1), *Nos2* (Mm00440502_m1), *Il1b* (Mm00434228_m1), *Ccl2* (Mm00441242_m1), *Il6* (Mm00446190_m1), *Egfr* (Mm01187858_m1), *Tgfa* (Mm00446232_m1), *Areg* (Mm00437583_m1), *Cxcl10* (Mm00445235_m1), *Cxcl2* (Mm00436450_m1), *Nfkbia* (Mm00477798_m1), *Tnfaip3* (Mm00437121_m1), *Il33* (Mm00505403_m1), and *Actb* (Mm02619580_g1). qPCR data were analyzed by the ddCt method by normalizing the expression of each gene for each replicate to *Gapdh* and then to the control group.

Western blotting

Western blotting was performed largely as described previously (*12, 13, 27, 37, 81*). Protein lysates were prepared by lysing cells with boiling 1X Laemmli buffer (Boston BioProducts, #BP-111R) followed by boiling at 95C for 5 minutes. SDS-PAGE was performed using Bolt 4-12% Bis-Tris Plus gradient gels (Invitrogen, #NW04125BOX). Western blotting was performed by transferring proteins onto a PVDF membrane (Millipore, #IPVH15150) in 1X NuPAGE buffer (Thermo Fisher, #NP00061). Membranes were blocked in 10% milk (Lab Scientific, #M0841) in TBS-T (Boston BioProducts, #IBB-180-2L). Primary antibodies used in this study are: goat anti-AREG (R&D Systems, #AF989, 0.1 µg/mL) and rabbit anti-GAPDH (Cell Signaling Technology, #2118S, 1:1000). The secondary antibodies used in this study are: anti-goat IgG H&L (HRP) (Abcam, #ab6741, 1:1000) and anti-rabbit IgG-HRP conjugate (Cell Signaling Technology, #7074S, 1:1000). Blots were imaged using an iBright CL1500 Imaging System

(Thermo Fisher).

Immunostaining of human CNS tissue

For immunostaining of paraffin sections, sections were deparaffinized in 2 washes of Xylenes (#214736, Sigma-Aldrich), followed by 2 washes in 100% EtOH for 5 minutes, 1 wash in 95% EtOH for 5 minutes, 1 wash in 70% EtOH for 5 minutes, 1 wash in 50% EtOH for 5 minutes, and then slides were rinsed with ddH2O. Antigen retrieval was performed by placing slides in boiling Epitope Retrieval Solution (#IW-11000, IHC World) for 20 minutes. Slides were dried, a hydrophobic barrier was made (#H-4000, Vector Laboratories) and sections were washed 3X for 5 minutes with 0.3% Triton X-100 in PBS (PBS-T). Sections were blocked with 5% donkey serum (#D9663, Sigma-Aldrich) in 0.3% PBS-T at RT for 30 minutes. Sections were then incubated with primary antibody diluted in blocking buffer overnight at 4C. Following primary antibody incubation, sections were washed 3X with 0.3% PBS-T and incubated with secondary antibody diluted in blocking buffer for 2 hours at RT. Sections were then washed 3X with 0.3% PBS-T, dried, and coverslips were mounted. Primary antibodies used in this study were: mouse anti-human TMEM119 (Novus Biologicals, #NBP2-76985, 1:200), goat anti-human AREG (R&D Systems, #AF262, 10µg/mL), GFAP-Cy3 (Sigma, #C9205, 1:500), and goat anti-human IL-33 (R&D Systems, #AF3625). Secondary antibodies used in this study were: Goat anti-mouse IgG (H+L) Cross-Adsorbed Secondary Antibody, Alexa Fluor 405 (Thermo Fisher, #A-31553), Donkey anti-goat IgG (H+L) Cross-Adsorbed Secondary Antibody, Alexa Fluor 488 (Invitrogen, #A-11055) both used at 1:500. Secondary antibodies were stained sequentially followed by 7X washes with PBS-T (anti-goat then anti-mouse) to avoid cross-reactivity. Human brain tissue was obtained from patients diagnosed with clinical and neuropathological MS diagnosis according to

the revised 2017 McDonald's criteria (*83*). Tissue samples were collected from healthy donors and MS patients with full ethical approval and informed consent as approved by the local ethics committee from the Centre de Recherche du Centre Hospitalier de l'Université de Montréal (CRCHUM) under ethical approval number BH07.001, Nagano 20.332-YP. Autopsy samples were preserved and lesions classified using luxol fast blue/H&E staining as previously published (*84, 85*).

FACS analysis of T cells

To analyze T cell populations, CNS and splenic cell suspensions were stimulated with 50 ng/mL phorbol 12-myristate 13-acetate (PMA, Sigma-Aldrich, #P8139), 1 μM Ionomycin (Sigma-Aldrich, # I3909-1ML), GolgiStop (BD Biosciences, #554724, 1:1500) and GolgiPlug (BD Biosciences, #555029, 1:1500) diluted in T cell culture medium (RPMI (Life Technologies, #11875119) containing 10% FBS, 1% penicillin/streptomycin, 50 μM 2-metcaptoethanol (Sigma-Aldrich, #M6250), and 1% non-essential amino acids (Life Technologies, #11140050)). After 4 hours, cell suspensions were washed with 0.5% BSA, 2 mM EDTA in 1X PBS and incubated with surface antibodies and a live/dead cell marker on ice. After 30 min, cells were washed with 0.5% BSA, 2mM EDTA in 1X PBS and fixed according to the manufacturer's protocol of an intracellular labeling kit (eBiosciences, #00-5523-00). Surface antibodies used in this study were: BUV661 anti-mouse CD45 (BD Biosciences, #565079, 1:100), BV750 anti-mouse CD3 (Biolegend, #100249, 1:50), PE-Cy7 anti-mouse CD4 (eBioscience, #25-0041-82, 1:100), BV785 anti-mouse CD11b (BD Biosciences, #101243, 1:100), BV570 anti-mouse Ly6C (Biolegend, #128030, 1:100), BUV805 anti-mouse CD8a (BD Bioscience, #564920, 1:100), BUV563 anti-mouse Ly6G (BD Biosciences, #565707, 1:100), BUV737 anti-mouse CD11c (BD Biosciences,

#612797, 1:100), Pe/Cy5 anti-mouse CD44 (BioLegend, #103010, 1:100), Intracellular antibodies were: APC anti-mouse IFN-γ (BD Biosciences, #554413, 1:100), PE anti-mouse IL-17A (eBiosciences, #12-7177-81, 1:100), BV421 anti-mouse GM-CSF (BD Biosciences, #564747, 1:100), FITC anti-mouse FoxP3 (eBiosciences, #11-5773-82, 1:100), biotinylated anti-mouse Areg (R&D Systems, #BAF989, 1:400), APC streptavidin (Biolegend, #405207, 1:500). AREG staining was performed as described previously (*42*). Gating of CNS and splenic cells was performed on >50,000 live $CD3^+CD4^+$ cells. FACs was performed on a Symphony A5 (BD Biosciences).

Isolation, culture, and stimulation of human primary astrocytes

Human fetal astrocytes were isolated from human CNS tissue (cerebral hemispheres) from fetuses at 17–23 weeks of gestation obtained from the Laboratory of Developmental Biology (Eunice Kennedy Shriver National Institute of Child Health and Human Development, project number: 5R24HD000836) following Canadian Institutes of Health Research–approved guidelines and cultured as previously described (*11-13, 30*). Astrocyte cultures were obtained by dissociation of the fetal CNS with 0.25% trypsin (Thermo Fisher Scientific, #25200-072) and 50 μg/mL DNase I (Roche, #10104159001) followed by mechanical dissociation. After washing, the cell suspension was plated at a concentration of $3\text{-}5*10^6$ cells/mL on poly-L-lysine (Sigma-Aldrich, #P4707) pre-coated 75 cm^2 flasks in DMEM supplemented with 10% FCS (#SH3007303, Fisher Scientific) and penicillin/streptomycin. To obtain pure astrocytes, the mixed CNS cell culture (containing astrocytes, microglia, and neurons) was passaged upon confluency, starting at 2 weeks post-isolation, using 0.25% trypsin-EDTA (Thermo Fisher Scientific, #25200-072). Human fetal astrocytes were passaged 2-4 times and purity (>90%) was determined by immunostaining using

rabbit anti-GFAP (Roche, #05269784001, 1:100) followed by goat anti-rabbit Texas Red IgG (Thermo Fisher Scientific, #T-2767, 1:100). The following compounds were used: 50 μg/ml poly(I:C) and human amphiregulin (R&D Systems, #262-AR-100). Cells were stimulated for 8 hours, cells were lysed in RLT buffer (Qiagen), and RNA processed analogous to mouse studies.

Bulk RNA-sequencing

Sorted cells were lysed and RNA isolated using the Qiagen RNeasy Micro kit (Qiagen, #74004) with on-column DNase I digestion (Qiagen, #79254). RNA was suspended in 10 μL of nuclease free water at 0.5-1 ng/μL and sequenced using SMARTSeq2(*86*) at the Broad Institute Technology Labs and the Broad Genomics Platform. Alternatively, bulk RNA was isolated from cells using the PicoPure RNA Isolation Kit (Thermo Fisher, #KIT0204) with on-column DNase digestion. RNA was then used as input with the NEBNext Low Input RNA Library Prep Kit (NEB, #E6420) according to the manufacturer's protocol. Reverse transcription was performed according to the SMART protocol using a template switching oligo. Then, cDNA was amplified and cleaned using Ampure XP beads (Beckman-Coulter, #A63881) and quantified using a Bioanalyzer DNA HS assay (Agilent, #50674626). Libraries were then fragmented, end-repaired, and ligated to Illumina compatible adaptors followed by sample barcoding using NEBNext Multiplex Oligos for Illumina (#E7335S, #E7500S, #7710S, #E7730S). Samples were selected again using Ampure XP beads and quantified using a Bioanalyzer. Libraries were quantified using a Kapa Library Quantification Kit (Kapa Biosystems, #KK4824) and run on an Illumina NextSeq550. Processed RNA-seq data was filtered by removing genes with low read counts. Read counts were normalized using TMM normalization and CPM (counts per million) were calculated to create a matrix of normalized expression values. The fastq files of each RNA-seq data sample were aligned to the

Mus musculus GRCm38 transcriptome using Kallisto (v0.46.1), and the same software was used to quantify the alignment results. Differential expression analysis was conducted using DESeq2, and the log2 fold change was adjusted using apeGLM for downstream analysis.

scRNA-seq analysis

For newly generated scRNA-seq data, multiplexed single cell datasets were processed using the CellRanger Pipeline 'multi' function to demultiplex and quantify samples (*87*). The filtered count matrix generated by CellRanger was used in the downstream analysis. Scrublet (*88*) was used to detect doublets in each sample. After detecting and removing doublets, cells in which we detected <500 or >2500 genes, >10,000 transcripts, or >25% mitochondrial content were filtered out before the analysis. The data were normalized using the negative binomial regression model with the top 4000 variable genes. Percentage mitochondrial content was regressed out in the normalization and scaling process (*89*). For analysis of a previously published dataset containing human microglia in MS and controls (*33*), fastq-files were processed using CellRanger Count using default settings. Seurat was used to cluster cells (*90*). Clusters expressing astrocyte markers from previous scRNA-seq studies were retained, with one cluster removed from downstream analyses. Cell type gene expression signature was calculated by using the following genes: astrocytes (*Aldh1l1*, *Aldoc*, *Apoe*, *Aqp4*, *Cd81*, *Gfap*, *Mfge8, S100b*, *Slc1a2*, and *Slc1a3*); oligodendrocytes (*Mag*, *Mbp*, and *Mog*); neurons (*Map2, Syt1*, and *Tubb3*); microglia (*Itgax, Spp1, Fam20c, Gpnmb, Apoc1, Fn1, Cxcr4*). To study the activation of IL-33 signaling in microglia, previously reported IL-33 signature genes were obtained (*91*) and a module signature score was calculated using the AddModuleScore in Seurat (*90*). All downstream differential expression analyses were conducted using MAST (*92*).

Bioinformatic analyses

Bioinformatic analysis of predicted upstream regulators and differentially regulated pathways was performed using Ingenuity Pathway Analysis (Qiagen) and gene set enrichment analysis (*93*). Gene sets used for signature scores are indicated in the corresponding figure. Previously published datasets were analyzed from the following studies at their respective accession numbers (*12, 27, 33-35, 78*). Venn diagram was created using nVenn (*94*).

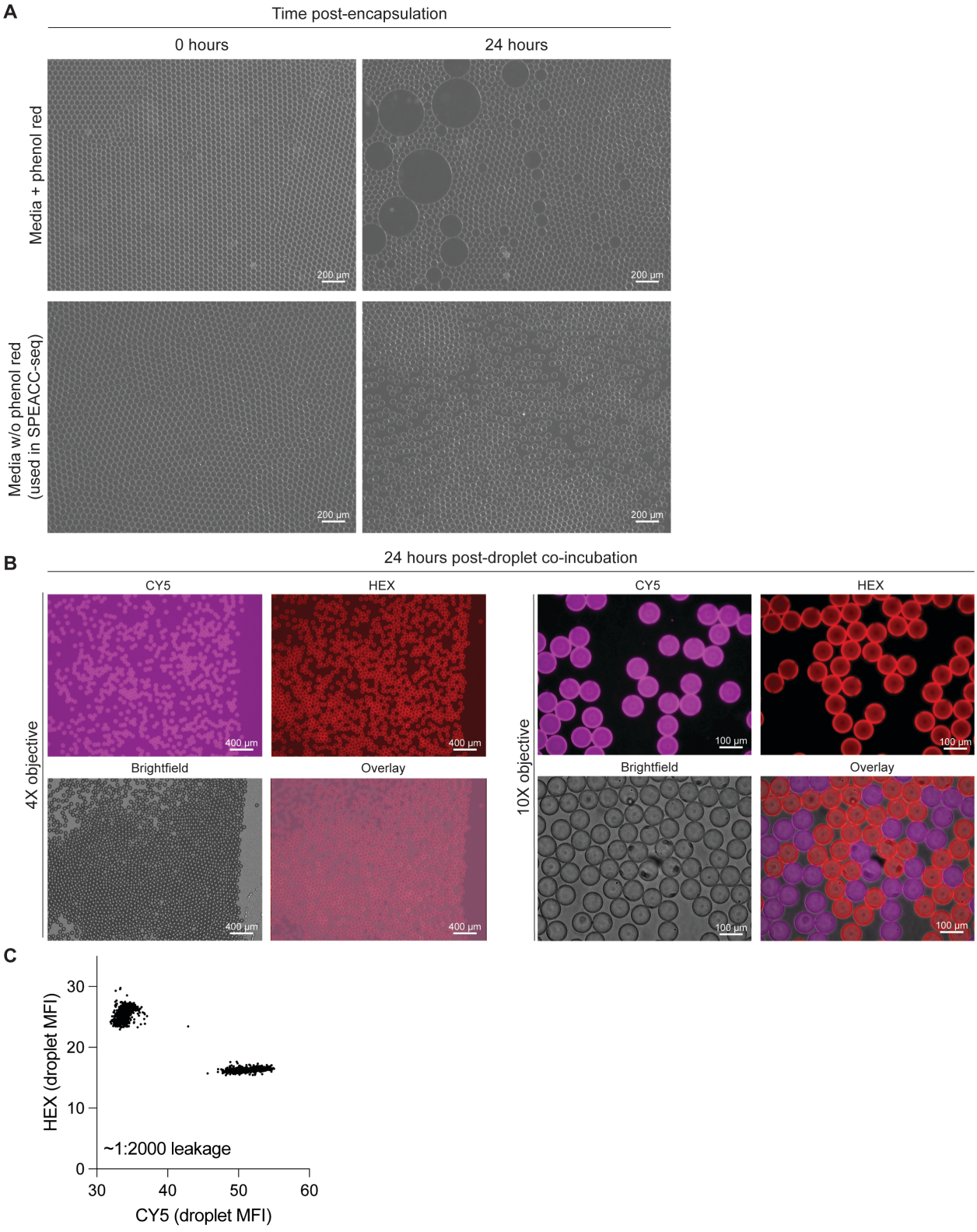
A
Time post-encapsulation
0 hours
24 hours
Media + phenol red
Media w/o phenol red (used in SPEACC-seq)
200 µm
B
24 hours post-droplet co-incubation
CY5
HEX
Brightfield
Overlay
4X objective
10X objective
400 µm
100 µm
C
HEX (droplet MFI)
CY5 (droplet MFI)
~1:2000 leakage
0
10
20
30
30
40
50
60

Fig. S1: Analysis of droplet stability. (A) Micrographs of droplets containing DMEM with (top) or without (bottom) phenol red. DMEM without phenol red was used for all SPEAC-seq studies. **(B)** Analysis of droplet leakage by fluorescence microscopy. Two independent droplet pools were generated, one containing HEX dye, and the other containing Cy5 dye. Droplet pools were mixed and cultured for 24-hours to assess dye leakage, which showed negligible leak. **(C)** Scatterplot quantifying dye leakage between droplets showing approximately 1:2,000 droplets contains both dyes in phenol red-free media after 24 hours of culture at 37C.

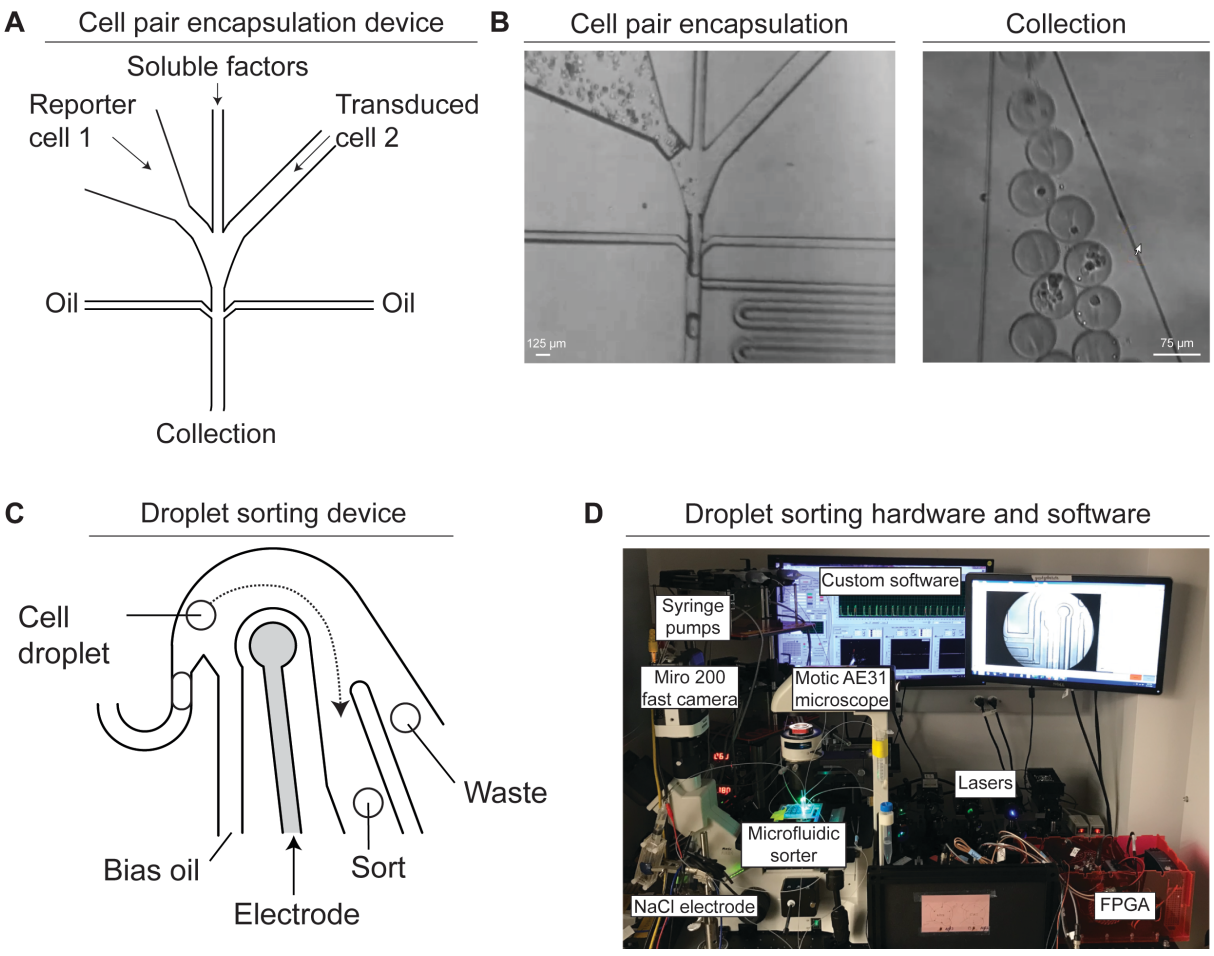
A
Cell pair encapsulation device
Soluble factors
Reporter cell 1
Transduced cell 2
Oil
Oil
Collection
B
Cell pair encapsulation
125 µm
Collection
75 µm
C
Droplet sorting device
Cell droplet
Waste
Bias oil
Sort
Electrode
D
Droplet sorting hardware and software
Custom software
Syringe pumps
Miro 200 fast camera
Motic AE31 microscope
Lasers
Microfluidic sorter
NaCl electrode
FPGA

Fig. S2: Microfluidic devices for cell pairing in droplets and droplet sorting. (A) Schematic of cell encapsulation co-flow device showing the location of cell and oil inlets. This device was used to encapsulate two distinct cell populations, those expressing: (i) a reporter and (ii) a perturbation derived from a CRISPR/Cas9 lentivirus library. Soluble factors (TNFα, IL-1β) were added using a central channel when desired. **(B)** Images of the co-flow device encapsulating cells (left), and the resulting droplets (right). **(C)** Schematic of the concentric droplet sorter showing the location of reinjected droplets, bias oil, sort electrode, and outlet channels. **(D)** Custom droplet cytometer and software for detecting, gating, and sorting drops containing cell pairs based on fluorescence.

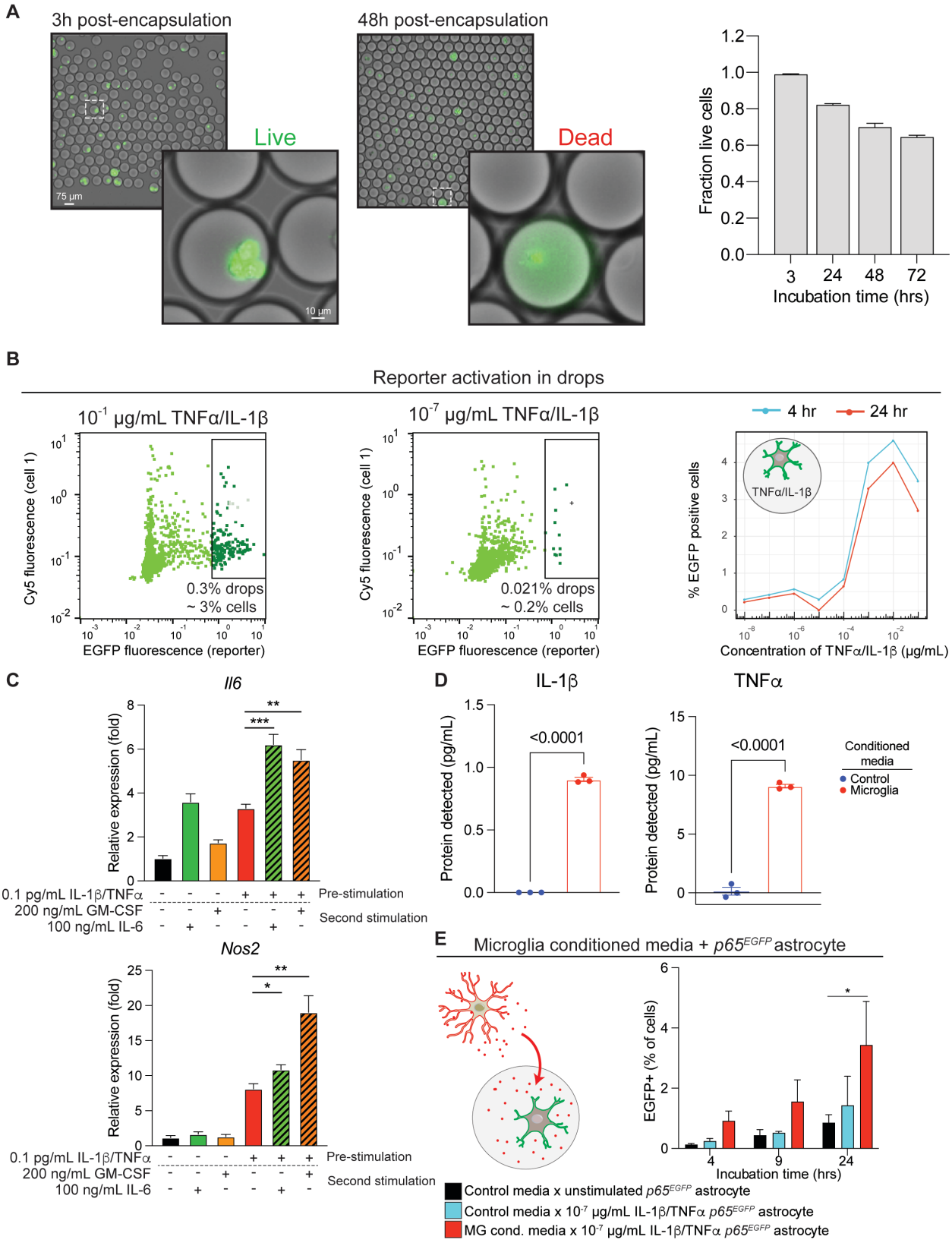
A
3h post-encapsulation
48h post-encapsulation
Live
Dead
75 µm
10 µm
Fraction live cells
Incubation time (hrs)
B
Reporter activation in drops
10-1 µg/mL TNFα/IL-1β
10-7 µg/mL TNFα/IL-1β
Cy5 fluorescence (cell 1)
EGFP fluorescence (reporter)
0.3% drops
~ 3% cells
0.021% drops
~ 0.2% cells
4 hr
24 hr
% EGFP positive cells
TNFα/IL-1β
Concentration of TNFα/IL-1β (µg/mL)
C
Il6
Nos2
Relative expression (fold)
0.1 pg/mL IL-1β/TNFα
200 ng/mL GM-CSF
100 ng/mL IL-6
Pre-stimulation
Second stimulation
D
IL-1β
TNFα
Protein detected (pg/mL)
<0.0001
Conditioned media
Control
Microglia
E
Microglia conditioned media + p65EGFP astrocyte
EGFP+ (% of cells)
Incubation time (hrs)
Control media x unstimulated p65EGFP astrocyte
Control media x 10-7 µg/mL IL-1β/TNFα p65EGFP astrocyte
MG cond. media x 10-7 µg/mL IL-1β/TNFα p65EGFP astrocyte

Fig. S3: Stimulation and monitoring of *p65^{EGFP}* astrocytes in droplets. (A) Representative images of primary astrocytes stained with calcein. Left picture: calcein is contained inside a live cell 4-hours post-encapsulation. Right picture: calcein leaks out of a dead cell 24 hours post-encapsulation. Quantification of primary astrocyte survival in droplets over a period of 72 hours. Calcein-stained cells were encapsulated in droplets, cultured for the indicated period of time, drops were broken, and cells were analyzed by FACS to measure the fraction of live cells. **(B)** Droplet cytometry of EGFP^{+} droplets following stimulation of *p65^{EGFP}* reporter astrocytes with 10^{-1} µg/mL (left) or 10^{-7} µg/mL (middle) TNFα and IL-1β at 24 hours post-encapsulation. Right: frequency of EGFP^{+} droplets as a function of TNFα and IL-1β concentration. **(C)** Analysis of pro-inflammatory cytokine expression upon a 24-h pre-stimulation with a subthreshold dose of IL-1β/TNFα (0.1 pg/mL) with or without subsequent IL-6 or GM-CSF stimulation. n=5-6 per condition. Unpaired two-tailed t-test. **(D)** Quantification of IL-1β and TNFα by ELISA in media conditioned by LPS-activated microglia. n=3 per group. Unpaired two-tailed t-test. **(E)** Frequency of EGFP^{+} droplets following co-incubation of sub-threshold stimulated or unstimulated *p65^{EGFP}* astrocytes with microglia conditioned media or control media at 4-, 9- and 24-hours post-encapsulation.

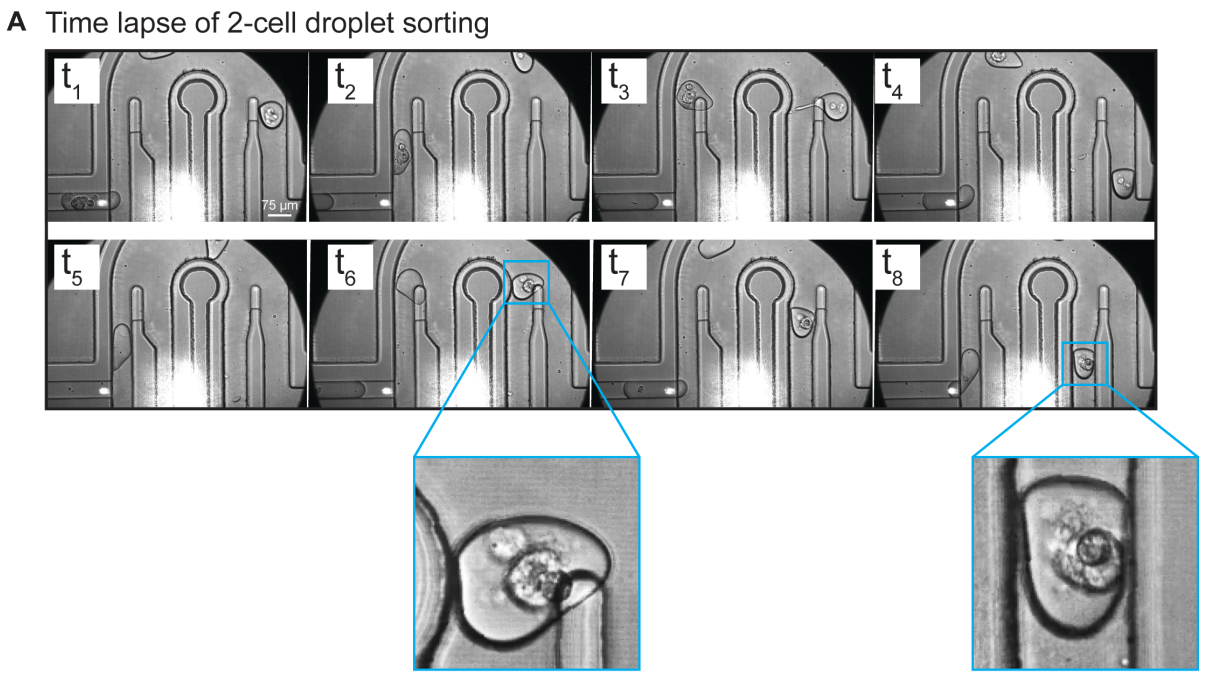
A
Time lapse of 2-cell droplet sorting
t1
t2
t3
t4
t5
t6
t7
t8
75 µm

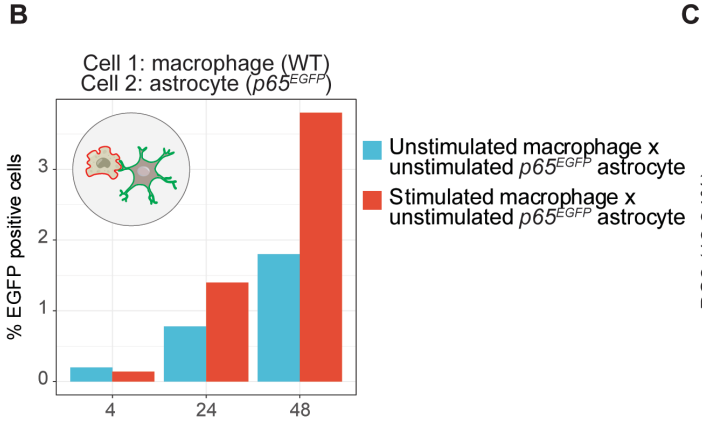
B
Cell 1: macrophage (WT)
Cell 2: astrocyte (p65EGFP)
% EGFP positive cells
0
1
2
3
4
24
48
Unstimulated macrophage x unstimulated p65EGFP astrocyte
Stimulated macrophage x unstimulated p65EGFP astrocyte

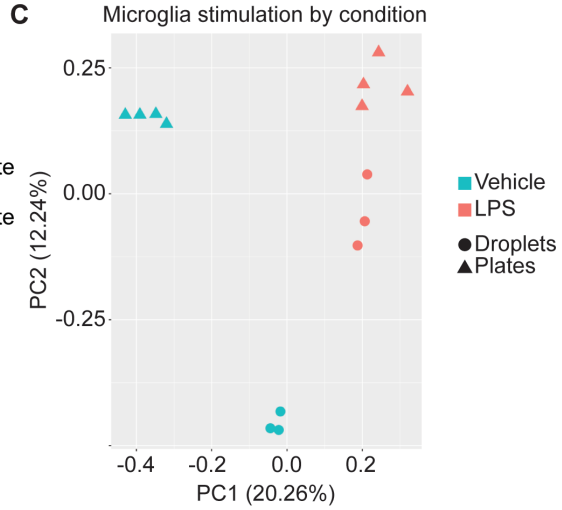
C
Microglia stimulation by condition
PC2 (12.24%)
0.25
0.00
-0.25
-0.4
-0.2
0.0
0.2
PC1 (20.26%)
Vehicle
LPS
Droplets
Plates

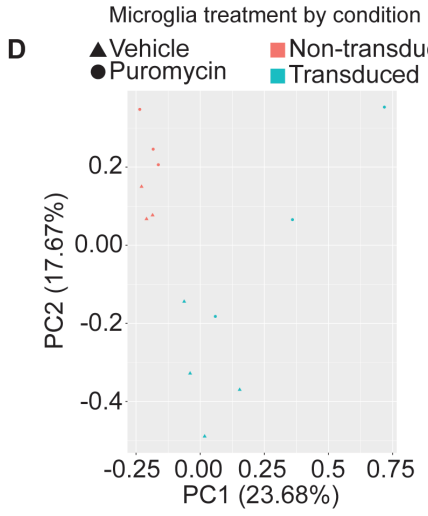
D
Microglia treatment by condition
Vehicle
Puromycin
Non-transduced
Transduced
PC2 (17.67%)
0.2
0.00
-0.2
-0.4
-0.25
0.00
0.25
0.5
0.75
PC1 (23.68%)

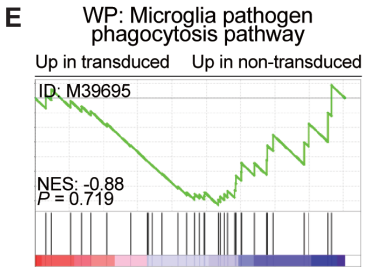
E
WP: Microglia pathogen phagocytosis pathway
Up in transduced
Up in non-transduced
ID: M39695
NES: -0.88
P = 0.719

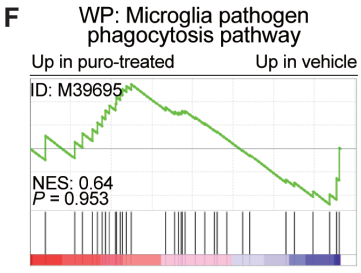
F
WP: Microglia pathogen phagocytosis pathway
Up in puro-treated
Up in vehicle
ID: M39695
NES: 0.64
P = 0.953

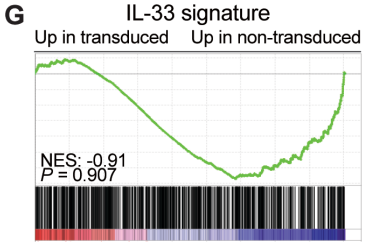
G
IL-33 signature
Up in transduced
Up in non-transduced
NES: -0.91
P = 0.907

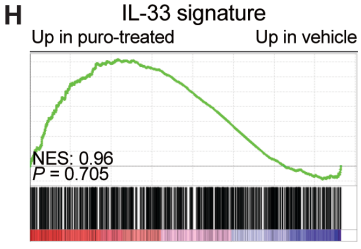
H
IL-33 signature
Up in puro-treated
Up in vehicle
NES: 0.96
P = 0.705

Fig. S4: Sorting interacting cells in droplets. (A) Time lapse images of the droplet sorter detecting and sorting cell pairs in droplets. **(B)** Frequency of EGFP+ droplets following co-incubation of *p65*^{EGFP} reporter astrocytes with LPS-pre-stimulated or unstimulated macrophages 4-, 24- and 48-hours post-encapsulation. **(C)** Principal component analysis of primary mouse microglia stimulated with LPS in plates or droplets. n=3-4 per group. **(D-H)** Analysis of microglial phagocytic pathways by PCA (D) or GSEA (E-H) in transduced or non-transduced microglia (D) or puromycin- or vehicle-treated primary mouse microglia (E) analyzed by RNA-seq. n=3 per group.

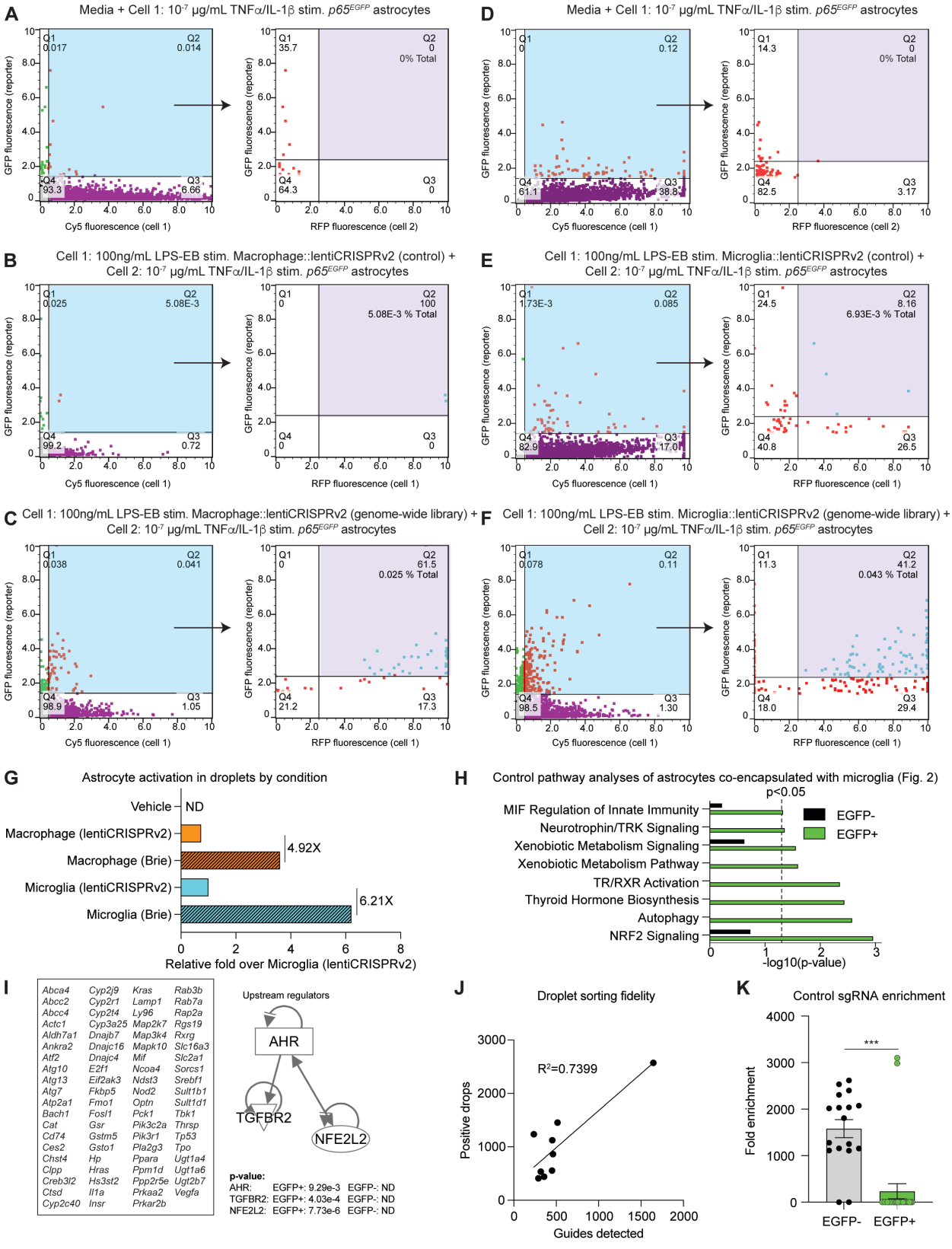
A
Media + Cell 1: 10-7 µg/mL TNFα/IL-1β stim. p65EGFP astrocytes
Q1 0.017
Q2 0.014
Q4 93.3
Q3 6.66
Q1 35.7
Q2 0 0% Total
Q4 64.3
Q3 0
GFP fluorescence (reporter)
Cy5 fluorescence (cell 1)
RFP fluorescence (cell 2)
B
Cell 1: 100ng/mL LPS-EB stim. Macrophage::lentiCRISPRv2 (control) + Cell 2: 10-7 µg/mL TNFα/IL-1β stim. p65EGFP astrocytes
Q1 0.025
Q2 5.08E-3
Q4 99.2
Q3 0.72
Q1 0
Q2 100 5.08E-3 % Total
Q4 0
Q3 0
C
Cell 1: 100ng/mL LPS-EB stim. Macrophage::lentiCRISPRv2 (genome-wide library) + Cell 2: 10-7 µg/mL TNFα/IL-1β stim. p65EGFP astrocytes
Q1 0.038
Q2 0.041
Q4 98.9
Q3 1.05
Q1 0
Q2 61.5 0.025 % Total
Q4 21.2
Q3 17.3
D
Media + Cell 1: 10-7 µg/mL TNFα/IL-1β stim. p65EGFP astrocytes
Q1 0
Q2 0.12
Q4 61.1
Q3 38.8
Q1 14.3
Q2 0 0% Total
Q4 82.5
Q3 3.17
E
Cell 1: 100ng/mL LPS-EB stim. Microglia::lentiCRISPRv2 (control) + Cell 2: 10-7 µg/mL TNFα/IL-1β stim. p65EGFP astrocytes
Q1 1.73E-3
Q2 0.085
Q4 82.9
Q3 17.0
Q1 24.5
Q2 8.16 6.93E-3 % Total
Q4 40.8
Q3 26.5
F
Cell 1: 100ng/mL LPS-EB stim. Microglia::lentiCRISPRv2 (genome-wide library) + Cell 2: 10-7 µg/mL TNFα/IL-1β stim. p65EGFP astrocytes
Q1 0.078
Q2 0.11
Q4 98.5
Q3 1.30
Q1 11.3
Q2 41.2 0.043 % Total
Q4 18.0
Q3 29.4
G
Astrocyte activation in droplets by condition
Vehicle
Macrophage (lentiCRISPRv2)
Macrophage (Brie)
Microglia (lentiCRISPRv2)
Microglia (Brie)
ND
4.92X
6.21X
Relative fold over Microglia (lentiCRISPRv2)
H
Control pathway analyses of astrocytes co-encapsulated with microglia (Fig. 2)
p<0.05
MIF Regulation of Innate Immunity
Neurotrophin/TRK Signaling
Xenobiotic Metabolism Signaling
Xenobiotic Metabolism Pathway
TR/RXR Activation
Thyroid Hormone Biosynthesis
Autophagy
NRF2 Signaling
EGFP-
EGFP+
-log10(p-value)
I
Abca4 Abcc2 Abcc4 Actc1 Aldh7a1 Ankra2 Atf2 Atg10 Atg13 Atg7 Atp2a1 Bach1 Cat Cd74 Ces2 Chst4 Clpp Creb3l2 Ctsd Cyp2c40
Cyp2j9 Cyp2r1 Cyp2t4 Cyp3a25 Dnajb7 Dnajc16 Dnajc4 E2f1 Eif2ak3 Fkbp5 Fmo1 Fosl1 Gsr Gstm5 Gsto1 Hp Hras Hs3st2 Il1a Insr
Kras Lamp1 Ly96 Map2k7 Map3k4 Mapk10 Mif Ncoa4 Ndst3 Nod2 Optn Pck1 Pik3c2a Pik3r1 Pla2g3 Ppara Ppm1d Ppp2r5e Prkaa2 Prkar2b
Rab3b Rab7a Rap2a Rgs19 Rxrg Slc16a3 Slc2a1 Sorcs1 Srebf1 Sult1b1 Sult1d1 Tbk1 Thrsp Tp53 Tpo Ugt1a4 Ugt1a6 Ugt2b7 Vegfa
Upstream regulators
AHR
TGFBR2
NFE2L2
p-value:
AHR: EGFP+: 9.29e-3 EGFP-: ND
TGFBR2: EGFP+: 4.03e-4 EGFP-: ND
NFE2L2: EGFP+: 7.73e-6 EGFP-: ND
J
Droplet sorting fidelity
R²=0.7399
Positive drops
Guides detected
K
Control sgRNA enrichment
***
Fold enrichment
EGFP-
EGFP+

Fig. S5: Droplet screening control data. (A-F) Droplet cytometry plots showing the gating strategy for unstimulated or non-targeting controls (A-B) and experimental (C) macrophage conditions as well as unstimulated or non-targeting controls (D-E) and experimental (F) microglia conditions at 24-hours post-encapsulation. Left gate: EGFP+ cells. Right gate: paired cells in droplets. **(G)** Quantification of the relative activation of reporter cells in droplets containing cell pairs that consist of macrophages or microglia together with astrocytes. **(H)** Analysis of anti-inflammatory pathways differentially activated in EGFP+ versus EGFP- fractions of $p65^{EGFP}$ reporter astrocytes co-encapsulated with a perturbed microglial cell. **(I)** Predicted upstream regulators and their transcriptional modules differentially expressed in EGFP+ versus EGFP- fractions of $p65^{EGFP}$ reporter astrocytes co-encapsulated with a perturbed microglial cell. **(J)** Scatterplot of the number of guides detected and the number of drops sorted for SPEAC-seq experiments. n=9 experiments. **(K)** Quantification of fold enrichment of non-targeting sgRNAs detected in each of the EGFP+ or EGFP- fractions of $p65^{EGFP}$ reporter astrocytes co-encapsulated with a perturbed microglial cell. n=17-26 sgRNAs per group. Unpaired two-tailed t-test.

A Cell 1: CRISPR/Cas9 *p65*^{EGFP} 10^{-7} µg/mL TNFα/IL-1β stim. astrocyte + Cell 2: 100 ng/mL LPS-EB stim. WT macrophage

Input drops: 1,160,000
Perturbed cells: 160,000
Drops sorted: 537
Guides detected: 318

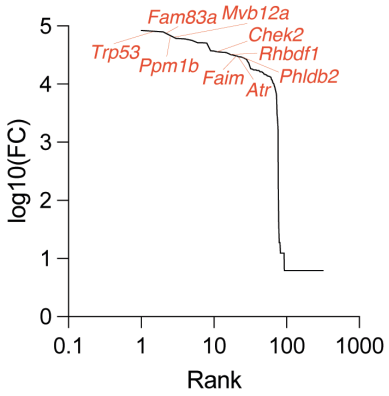

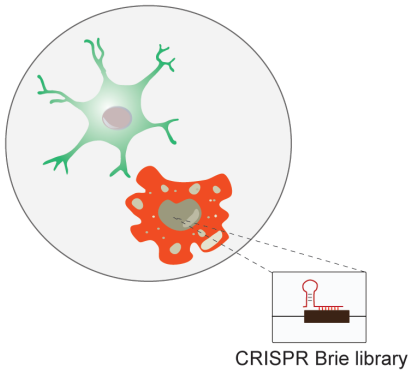

B Cell 1: *p65*^{EGFP} 10^{-7} µg/mL TNFα/IL-1β stim. astrocyte + Cell 2: 100 ng/mL TNFα/IL-1β stim. CRISPR/Cas9 WT astrocyte

Input drops: 860,000
Perturbed cells: 86,000
Drops sorted: 555
Guides detected: 451

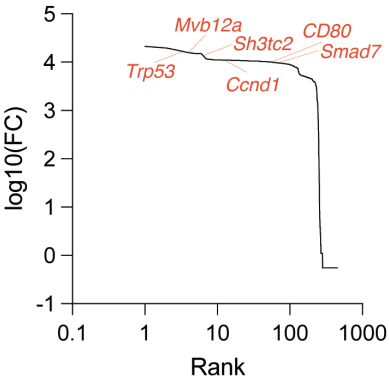

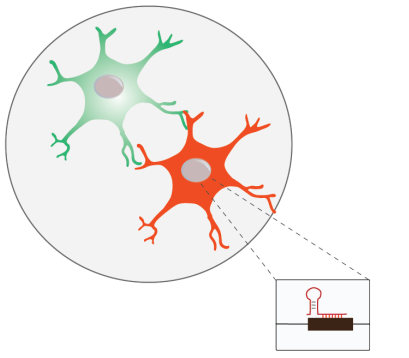

C Cell 1: CRISPR/Cas9 *p65*^{EGFP} 10^{-7} µg/mL TNFα/IL-1β stim. astrocyte + Cell 2: 100 ng/mL LPS-EB stim. WT macrophage

Input drops: 1,000,000
Perturbed cells: 100,000
Drops sorted: 411
Guides detected: 290

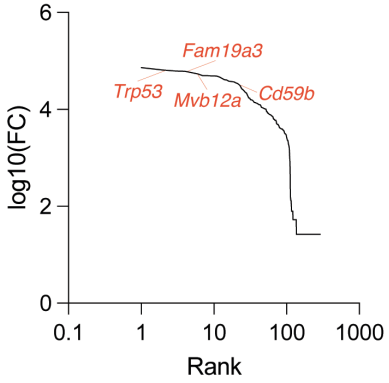

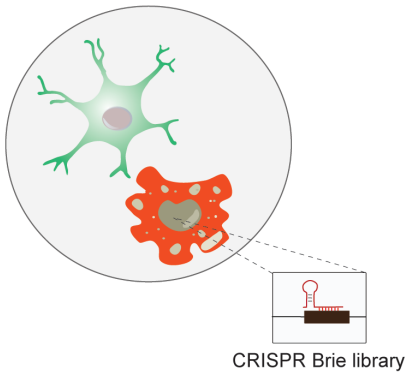

Fig. S6: Droplet CRISPR screens with *p65^{EGFP}* reporter astrocytes. (A-C) Left: Identification of genes in positive (EGFP+) droplets. Middle: Schematic of the stimulation and pairing scheme. Right: Gene ontology analysis of hits identified in each screen. *p65^{EGFP}* reporter astrocytes were incubated under the following conditions. Partner cells were transduced with a genome-wide CRISPR/Cas9 lentiviral library: (A) stimulated bone marrow-derived macrophages (24-hr of 100 ng/mL LPS-EB); (B) stimulated (24hr of 100 ng/mL TNFα/IL-1β) astrocytes; (C) stimulated bone marrow-derived macrophages (24-hr of 100 ng/mL LPS-EB).

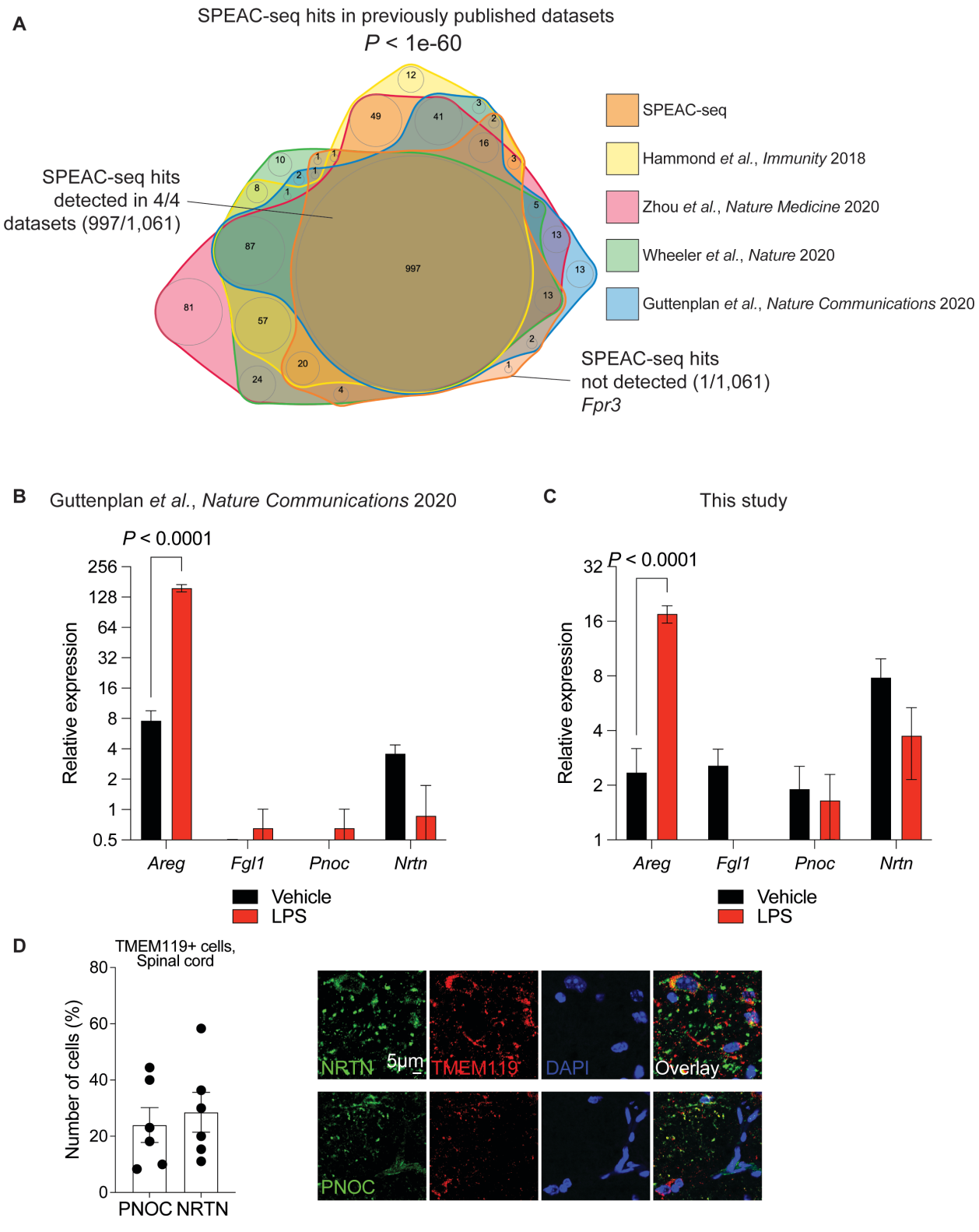
A
SPEAC-seq hits in previously published datasets
P < 1e-60
SPEAC-seq hits detected in 4/4 datasets (997/1,061)
SPEAC-seq hits not detected (1/1,061) Fpr3
SPEAC-seq
Hammond et al., Immunity 2018
Zhou et al., Nature Medicine 2020
Wheeler et al., Nature 2020
Guttenplan et al., Nature Communications 2020
B
Guttenplan et al., Nature Communications 2020
P < 0.0001
Relative expression
Areg
Fgl1
Pnoc
Nrtn
Vehicle
LPS
C
This study
P < 0.0001
Relative expression
Areg
Fgl1
Pnoc
Nrtn
Vehicle
LPS
D
TMEM119+ cells, Spinal cord
Number of cells (%)
PNOC NRTN
NRTN
5μm
TMEM119
DAPI
Overlay
PNOC

Fig. S7: Validation of microglial SPEAC-seq hits in independent datasets. (A) Venn diagram depicting the overlap of filtered SPEAC-seq hits filtered based on RNA expression from Fig. 2F with 4 independent bulk or single-cell RNA-seq datasets of microglia that were previously published (*27, 34, 35, 78*). **(B-C)** Analysis of gene expression for the candidate factors *Areg*, *Fgl1*, *Pnoc*, and *Nrtn* obtained by Guttenplan *et al.*, in (*78*) (n=3 per group) or analyzed in this study (n=4 per group). **(D)** Quantification of PNOC and NRTN in TMEM119+ cells in naïve mice spinal cords. n=6 images from N=3 mice.

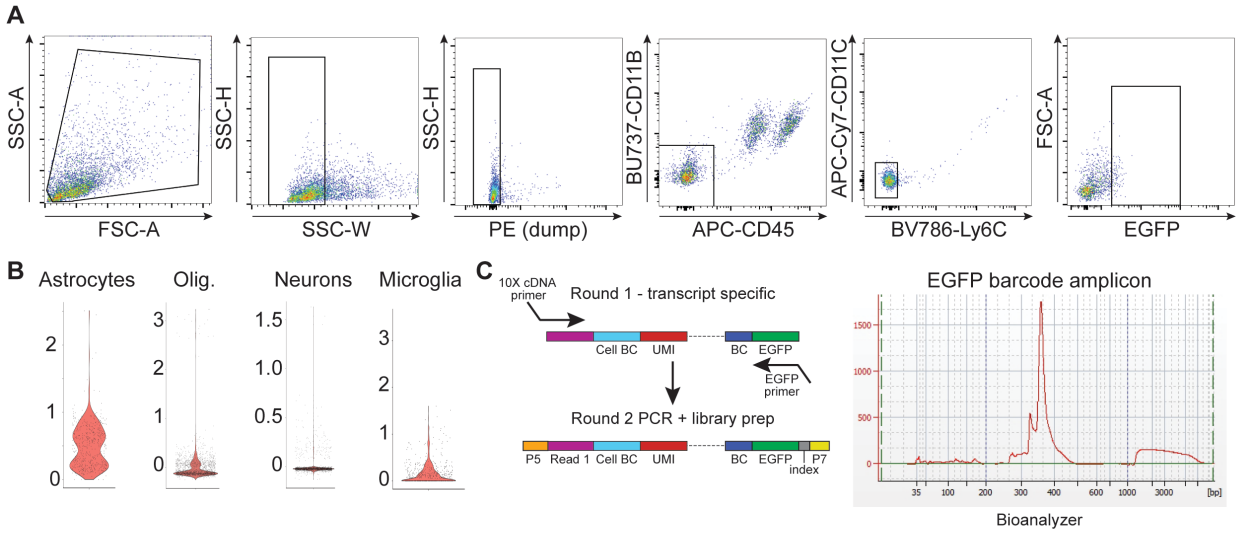

D

TNFα+IL-1β regulatory networks

sgGfra2

z-score: TNF: -1.755, IL-1β: ND
p-value: TNF: 0.0348, IL-1β: ND

sgLag3

z-score: TNF: -0.712, IL-1β: -0.549
p-value: TNF: 1.63e-6, IL-1β: 7.45e-5

sgOprl1

z-score: TNF: -0.384, IL-1β: 0.015
p-value: TNF: 3.29e-6, IL1β: 0.0418

E

sgEgfr vs. others

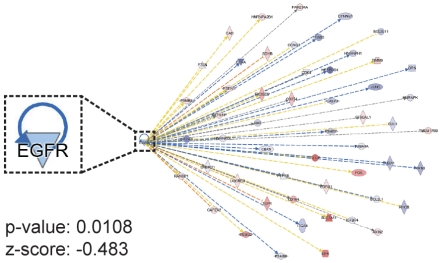

p-value: 0.0108
z-score: -0.483

F

Legend for all Qiagen IPA diagrams

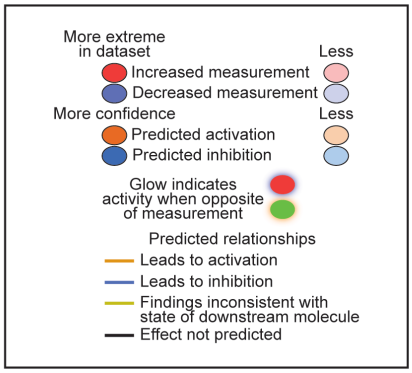

Fig. S8: Control analyses for Perturb-seq experiments. (A) Flow cytometry schematic used to sort EGFP+ astrocytes. **(B)** Cell type signature scores for barcode-expressing Perturb-seq cells. **(C)** Workflow for amplifying and detecting EGFP barcodes associated with a perturbation. **(D)** Predicted regulatory networks for IL-1β/TNFα as a function of each receptor perturbation in astrocyte Perturb-seq experiments. Please note the activation of IL-1β/TNFα signaling is highest when *sgEgfr* is perturbed. **(E)** Bioinformatic validation of *Egfr* knockdown in *sgEgfr*-perturbed cells. **(F)** Legend for all IPA diagrams contained in this study.

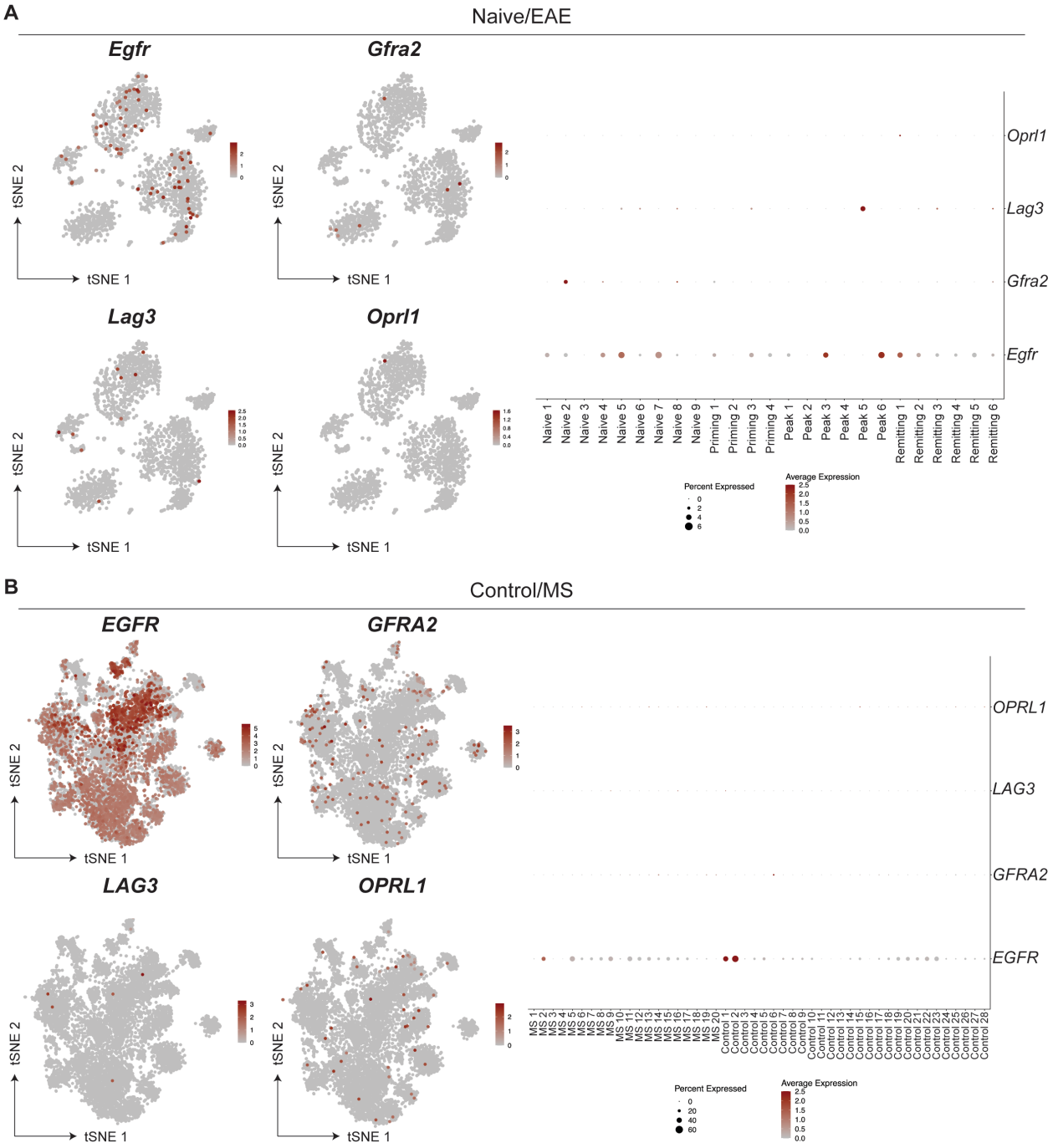
A
Naive/EAE
Egfr
Gfra2
Lag3
Oprl1
tSNE 1
tSNE 2
Oprl1
Lag3
Gfra2
Egfr
Naive 1
Naive 2
Naive 3
Naive 4
Naive 5
Naive 6
Naive 7
Naive 8
Naive 9
Priming 1
Priming 2
Priming 3
Priming 4
Peak 1
Peak 2
Peak 3
Peak 4
Peak 5
Peak 6
Remitting 1
Remitting 2
Remitting 3
Remitting 4
Remitting 5
Remitting 6
Percent Expressed
Average Expression
B
Control/MS
EGFR
GFRA2
LAG3
OPRL1
OPRL1
LAG3
GFRA2
EGFR
Percent Expressed
Average Expression

Fig. S9: Receptor expression in astrocytes in EAE and MS. (A-B) Expression of each perturbed receptor in astrocytes (n=25 mice) during EAE (A) and in MS or control patients (n=48) (B) previously reported in (*27*), shown as overall tSNE plots (left) or in pseudobulk analyses by patient (right).

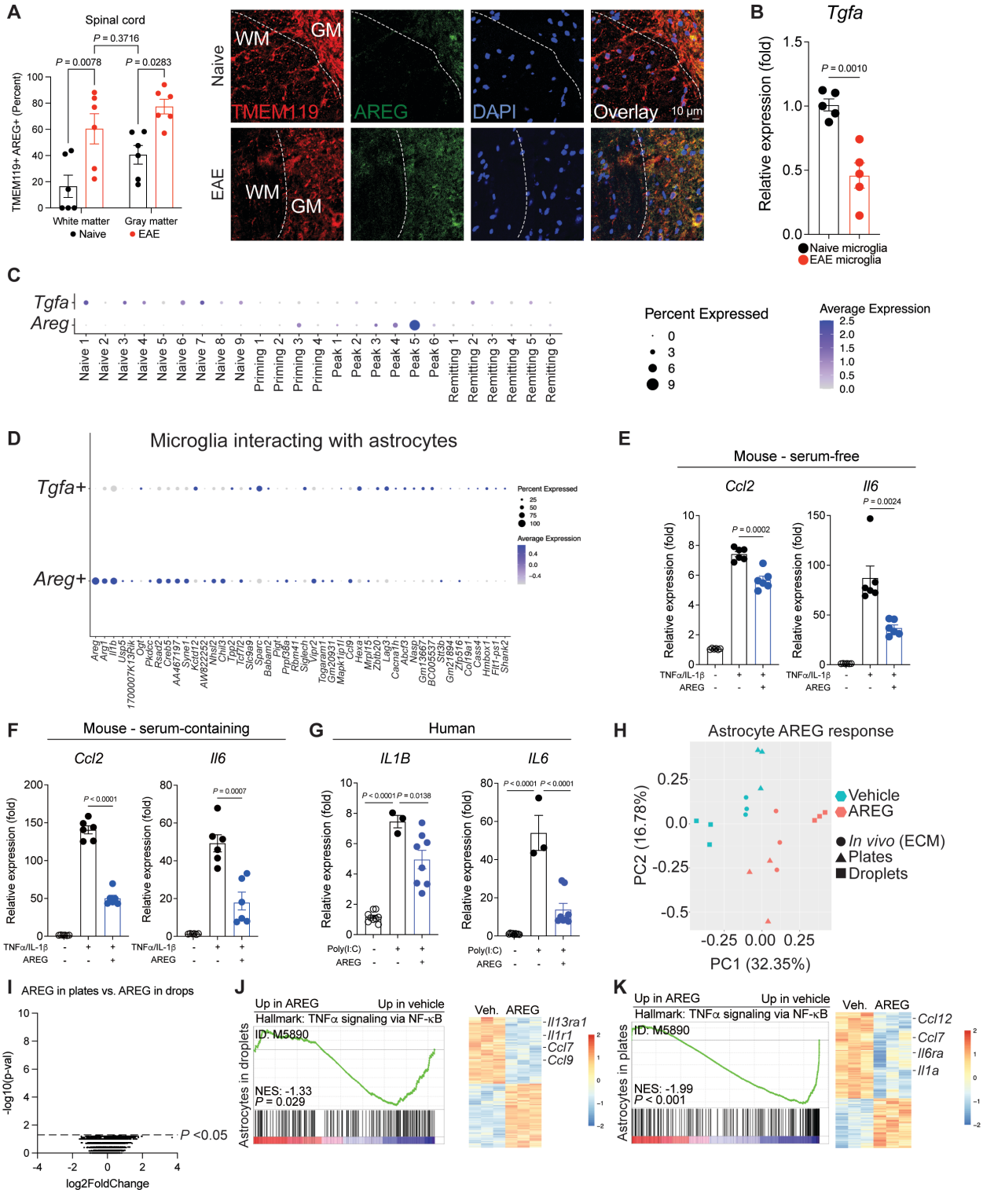
A
Spinal cord
P = 0.3716
P = 0.0078
P = 0.0283
TMEM119+ AREG+ (Percent)
White matter
Gray matter
Naive
EAE
WM
GM
TMEM119
AREG
DAPI
Overlay
10 μm
B
Tgfa
P = 0.0010
Relative expression (fold)
Naive microglia
EAE microglia
C
Tgfa
Areg
Percent Expressed
Average Expression
D
Microglia interacting with astrocytes
Tgfa+
Areg+
E
Mouse - serum-free
Ccl2
Il6
P = 0.0002
P = 0.0024
TNFα/IL-1β
AREG
F
Mouse - serum-containing
P < 0.0001
P = 0.0007
G
Human
IL1B
IL6
P = 0.0138
Poly(I:C)
H
Astrocyte AREG response
PC1 (32.35%)
PC2 (16.78%)
Vehicle
AREG
In vivo (ECM)
Plates
Droplets
I
AREG in plates vs. AREG in drops
-log10(p-val)
log2FoldChange
P <0.05
J
Up in AREG
Up in vehicle
Hallmark: TNFα signaling via NF-κB
ID: M5890
NES: -1.33
P = 0.029
Astrocytes in droplets
Veh.
AREG
Il13ra1
Il1r1
Ccl7
Ccl9
K
NES: -1.99
P < 0.001
Astrocytes in plates
Ccl12
Ccl7
Il6ra
Il1a

Fig. S10: *Areg*+ and *Tgfa*+ microglia are differentially regulated. (A) Analysis of AREG+ TMEM119+ microglia across the spinal cord by immunostaining. n=6 images from N=3 mice. Unpaired two-tailed t-test. **(B)** Quantification of *Tgfa* expression in microglia and astrocytes isolated from naïve or EAE mice. n=5 per group. Unpaired two-tailed t-test. **(C)** *Areg* or *Tgfa* expression shown by pseudobulk in microglia/macrophages over the course of EAE previously reported in (*27*). **(D)** Gene expression differences in *Areg*+ and *Tgfa*+ microglia interacting with astrocytes detected by RABID-seq previously reported in (*12*). **(E-G)** Analysis of pro-inflammatory cytokine expression in primary serum-free mouse (E), serum-containing mouse (F), or primary human astrocytes (G) as a function of cytokine and AREG treatment. n=3-9 per group. Unpaired two-tailed t-test. **(H)** Principal component analysis of astrocytes treated with AREG or vehicle in adherent culture, droplets, or intracranial injection and analyzed by RNA-seq. n=3 per group. **(I)** Analysis of astrocyte transcriptional responses to 10 ng/mL AREG in plates versus droplets. Data analyzed by calculating fold change of each treatment relative to control then testing for mean differences of each fold change. Wilcoxon signed-rank test. **(J-K)** GSEA analysis and heatmaps of AREG-treated astrocytes in droplets (I) or plates (J) showing comparable anti-inflammatory properties.

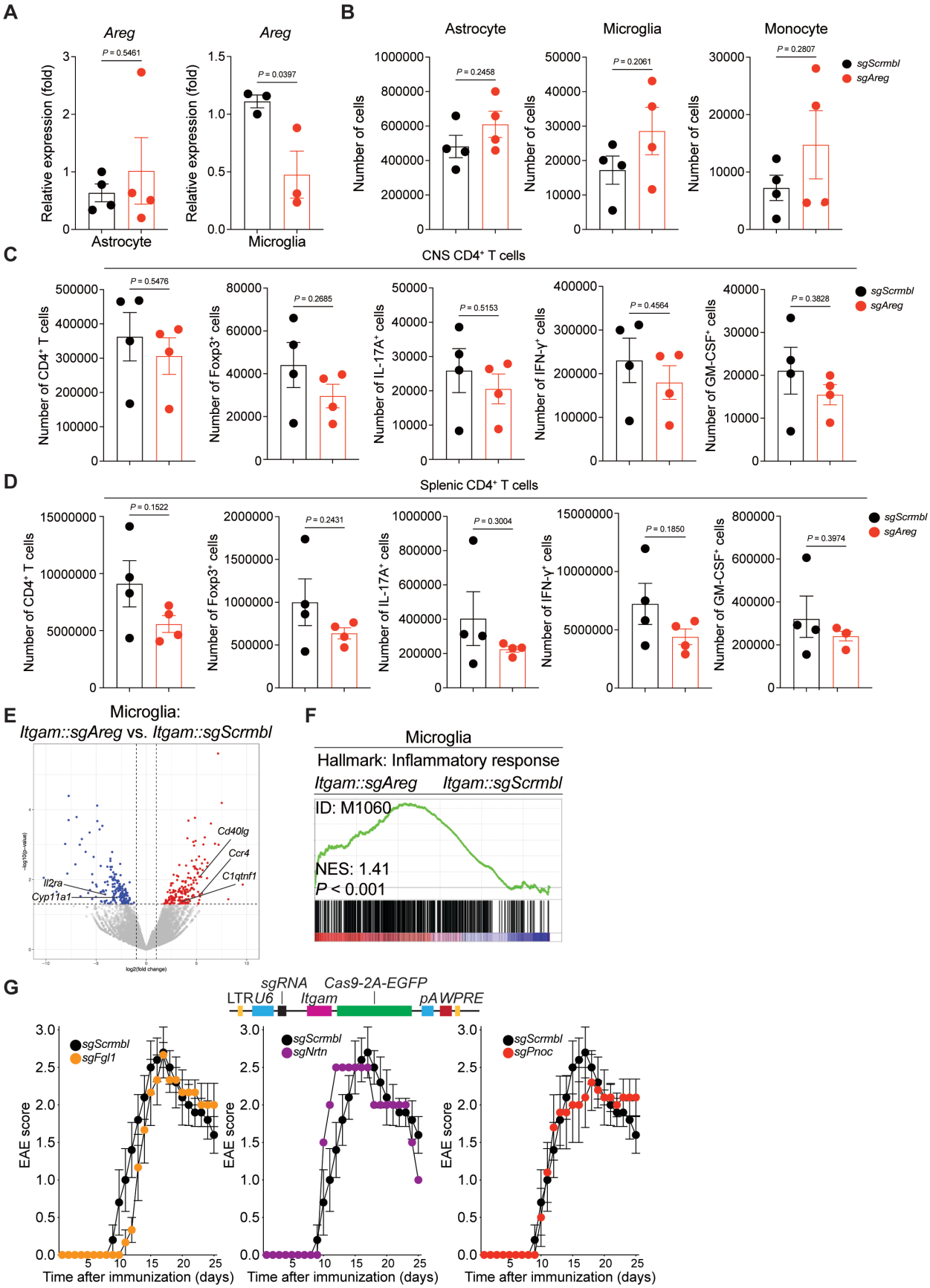
A
Areg
P = 0.5461
Relative expression (fold)
Astrocyte
Areg
P = 0.0397
Relative expression (fold)
Microglia
B
Astrocyte
P = 0.2458
Number of cells
Microglia
P = 0.2061
Number of cells
Monocyte
P = 0.2807
Number of cells
sgScrmbl
sgAreg
C
CNS CD4⁺ T cells
Number of CD4⁺ T cells
P = 0.5476
Number of Foxp3⁺ cells
P = 0.2685
Number of IL-17A⁺ cells
P = 0.5153
Number of IFN-γ⁺ cells
P = 0.4564
Number of GM-CSF⁺ cells
P = 0.3828
sgScrmbl
sgAreg
D
Splenic CD4⁺ T cells
Number of CD4⁺ T cells
P = 0.1522
Number of Foxp3⁺ cells
P = 0.2431
Number of IL-17A⁺ cells
P = 0.3004
Number of IFN-γ⁺ cells
P = 0.1850
Number of GM-CSF⁺ cells
P = 0.3974
sgScrmbl
sgAreg
E
Microglia:
Itgam::sgAreg vs. Itgam::sgScrmbl
Cd40lg
Ccr4
C1qtnf1
Il2ra
Cyp11a1
F
Microglia
Hallmark: Inflammatory response
Itgam::sgAreg
Itgam::sgScrmbl
ID: M1060
NES: 1.41
P < 0.001
G
sgRNA
Cas9-2A-EGFP
LTR
U6
Itgam
pA
WPRE
sgScrmbl
sgFgl1
sgScrmbl
sgNrtn
sgScrmbl
sgPnoc
EAE score
Time after immunization (days)

Fig. S11: Control analyses of the immune response following *Areg* knockdown. (A) Demonstration of *sgAreg* knockdown specificity in microglia compared to astrocytes. n=3-4 per group. Unpaired two-tailed t-test. **(B-D)** Quantification of astrocytes, microglia, and CNS-recruited monocytes (B), CNS-recruited (C) and splenic (D) T cells following *sgAreg* knockdown. n=4 per group. Unpaired two-tailed t-test. **(E-F)** RNA-seq analyses show increased inflammatory signatures in *sgAreg*-targeted microglia compared with controls. n=3 mice per group. **(G)** In vivo genetic perturbation screening of *Fgl1*, *Nrtn*, and *Pnoc* in microglia using an *Itgam*-driven Cas9-2A-EGFP lentiviral vector.

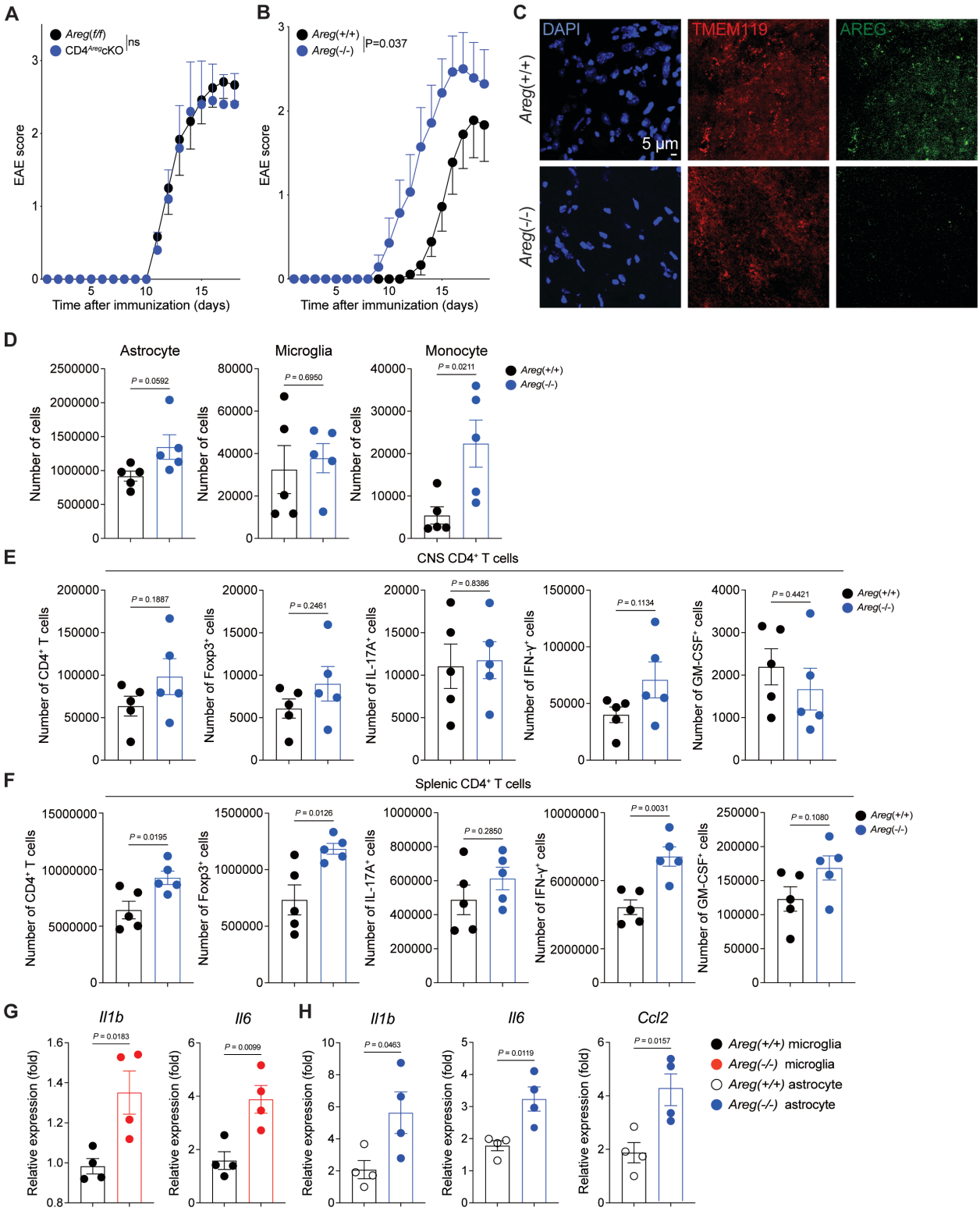
A
Areg(f/f)
CD4AregcKO
ns
EAE score
Time after immunization (days)
B
Areg(+/+)
Areg(-/-)
P=0.037
EAE score
Time after immunization (days)
C
DAPI
TMEM119
AREG
Areg(+/+)
Areg(-/-)
5 μm
D
Astrocyte
Microglia
Monocyte
Number of cells
P = 0.0592
P = 0.6950
P = 0.0211
Areg(+/+)
Areg(-/-)
E
CNS CD4+ T cells
Number of CD4+ T cells
Number of Foxp3+ cells
Number of IL-17A+ cells
Number of IFN-γ+ cells
Number of GM-CSF+ cells
P = 0.1887
P = 0.2461
P = 0.8386
P = 0.1134
P = 0.4421
Areg(+/+)
Areg(-/-)
F
Splenic CD4+ T cells
Number of CD4+ T cells
Number of Foxp3+ cells
Number of IL-17A+ cells
Number of IFN-γ+ cells
Number of GM-CSF+ cells
P = 0.0195
P = 0.0126
P = 0.2850
P = 0.0031
P = 0.1080
Areg(+/+)
Areg(-/-)
G
Il1b
Il6
Relative expression (fold)
P = 0.0183
P = 0.0099
H
Il1b
Il6
Ccl2
Relative expression (fold)
P = 0.0463
P = 0.0119
P = 0.0157
Areg(+/+) microglia
Areg(-/-) microglia
Areg(+/+) astrocyte
Areg(-/-) astrocyte

Fig. S12: Analysis of *Areg* germline KO mice. (A) EAE curve of *Cd4::Areg(f/f)* mice and *Areg(f/f)* controls. n=5-6 per group. Two-way repeated measures ANOVA. **(B)** EAE curve of *Areg-/-* mice n=7-9 per group. Two-way repeated measures ANOVA. **(C)** Validation of AREG KO by immunostaining. **(D-F)** Quantification of astrocytes, microglia, and CNS-recruited monocytes (D) as well as CNS-recruited (E) and splenic (F) T cells. n=5 per group. Unpaired two-tailed t-test. **(G-H)** Analysis by qPCR of pro-inflammatory gene expression in microglia (G) and astrocytes (H) isolated from *Areg-/-* mice. n=4 per group. Unpaired two-tailed t-test.

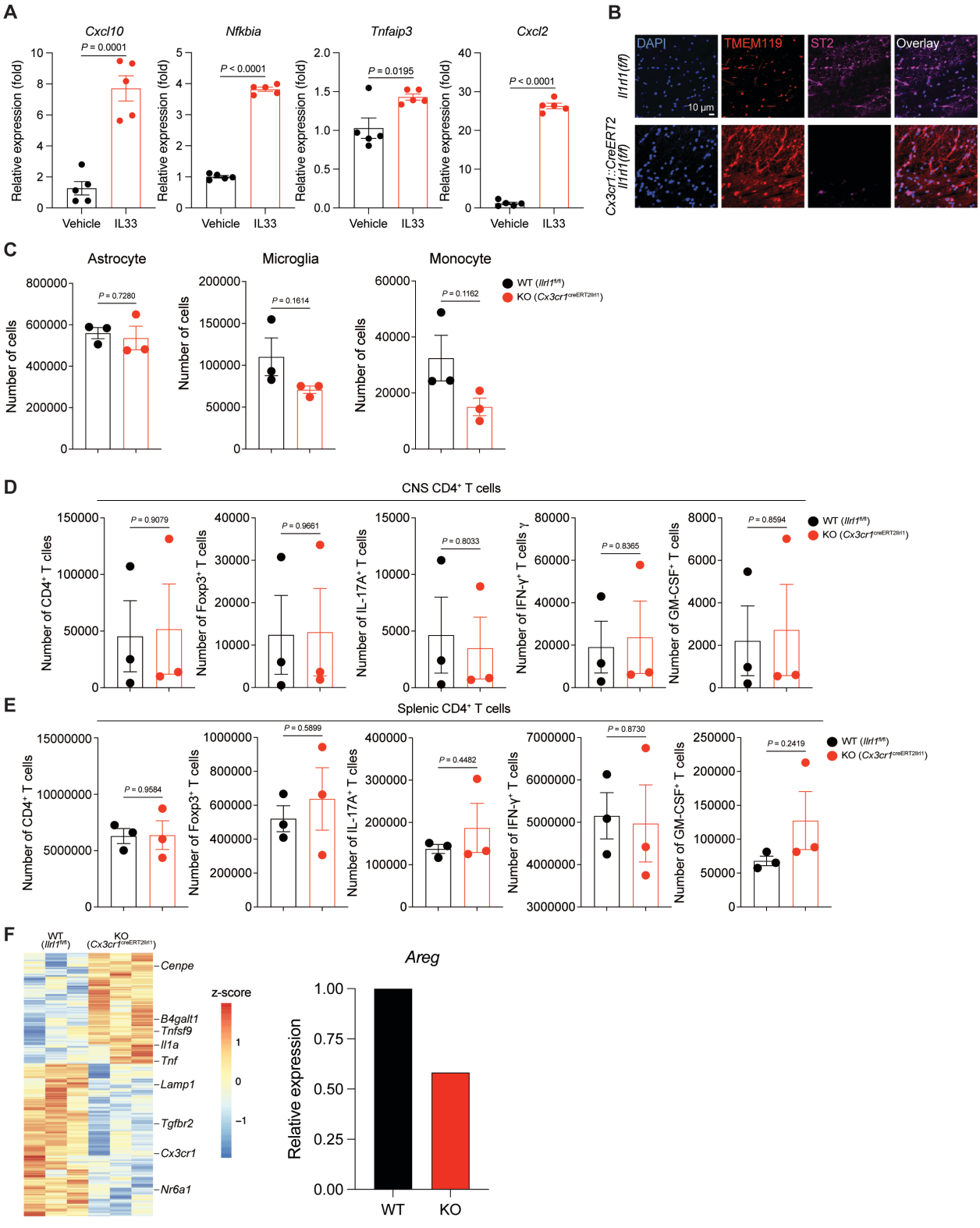
A
Cxcl10
P = 0.0001
Nfkbia
P < 0.0001
Tnfaip3
P = 0.0195
Cxcl2
P < 0.0001
Relative expression (fold)
Vehicle
IL33
B
DAPI
TMEM119
ST2
Overlay
10 μm
Il1r1(f/f)
Cx3cr1::CreERT2 Il1r1(f/f)
C
Astrocyte
Microglia
Monocyte
P = 0.7280
P = 0.1614
P = 0.1162
Number of cells
WT (Il1r1f/f)
KO (Cx3cr1creERT2Il1r1)
D
CNS CD4+ T cells
P = 0.9079
P = 0.9661
P = 0.8033
P = 0.8365
P = 0.8594
Number of CD4+ T clles
Number of Foxp3+ T cells
Number of IL-17A+ T clles
Number of IFN-γ+ T cells γ
Number of GM-CSF+ T cells
E
Splenic CD4+ T cells
P = 0.9584
P = 0.5899
P = 0.4482
P = 0.8730
P = 0.2419
Number of CD4+ T cells
Number of Foxp3+ T cells
Number of IL-17A+ T clles
Number of IFN-γ+ T cells
Number of GM-CSF+ T cells
F
WT (Il1r1f/f)
KO (Cx3cr1creERT2Il1r1)
Cenpe
B4galt1
Tnfsf9
Il1a
Tnf
Lamp1
Tgfbr2
Cx3cr1
Nr6a1
z-score
Areg
Relative expression
WT
KO

Fig. S13: Control of CNS inflammation by microglial ST2 signaling. (A) qPCR analysis of genes induced by IL-33 signaling. n=5 per group. Unpaired two-tailed t-test. **(B)** Immunostaining of ST2 in microglia demonstrating knockout in *Cx3cr1*::*CreERT2*;*Il1rl1*(*f/f*) mice. Representative image from N=3 mice. **(C-E)** Quantification of astrocytes, microglia, and CNS-recruited monocytes (C) as well as CNS-recruited (D) and splenic (E) T cells. n=3 per group. Unpaired two-tailed t-test. **(F)** RNA-seq analysis of microglia isolated from *Cx3cr1*::*CreERT2*;*Il1rl1*(*f/f*) mice. n=3 per group.

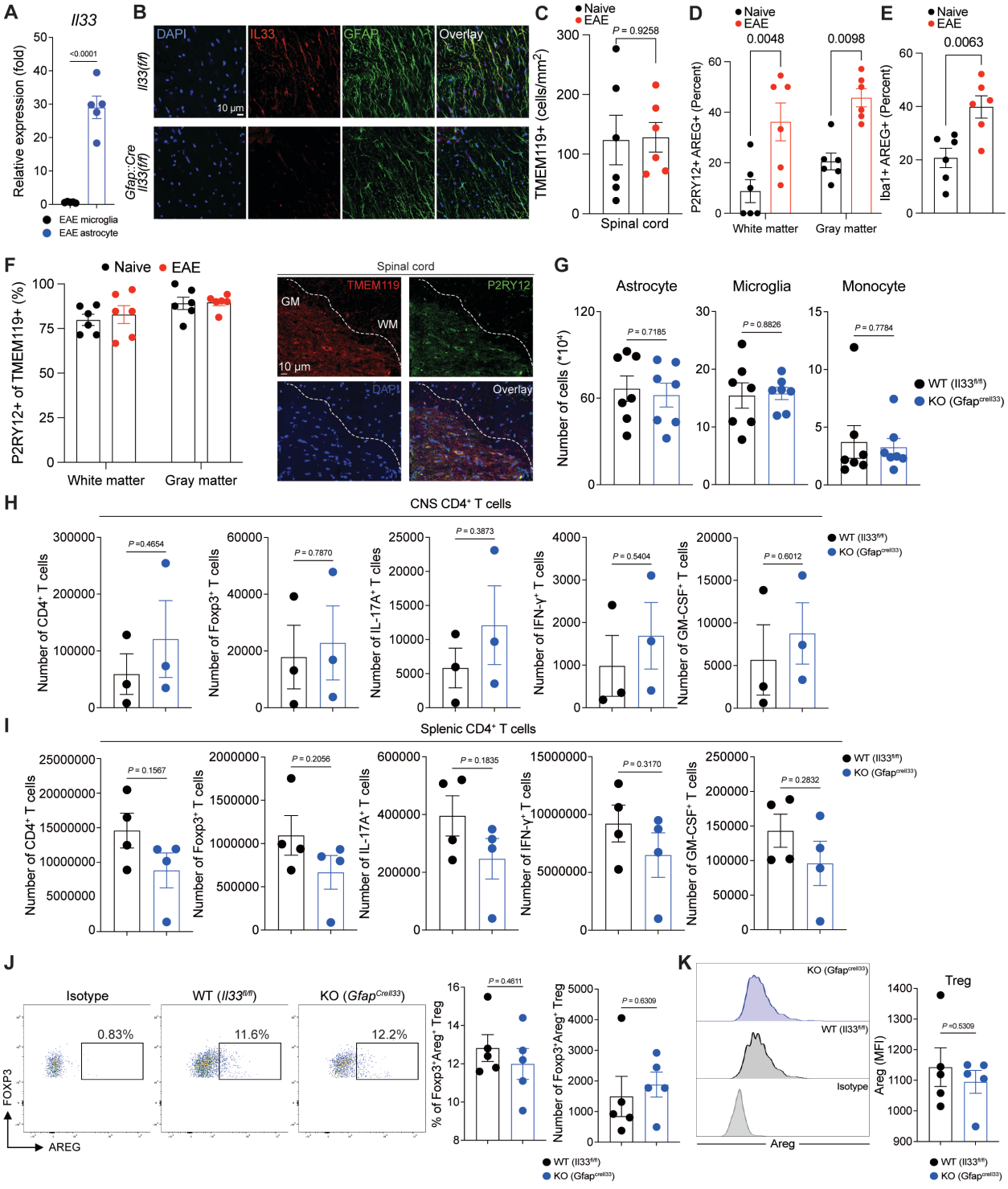
A
Il33
Relative expression (fold)
<0.0001
EAE microglia
EAE astrocyte
B
DAPI
IL33
GFAP
Overlay
Il33(f/f)
Gfap::Cre Il33(f/f)
10 μm
C
Naive
EAE
P = 0.9258
TMEM119+ (cells/mm2)
Spinal cord
D
Naive
EAE
0.0048
0.0098
P2RY12+ AREG+ (Percent)
White matter
Gray matter
E
Naive
EAE
0.0063
Iba1+ AREG+ (Percent)
F
Naive
EAE
P2RY12+ of TMEM119+ (%)
White matter
Gray matter
Spinal cord
TMEM119
P2RY12
GM
WM
10 μm
DAPI
Overlay
G
Astrocyte
Microglia
Monocyte
P = 0.7185
P = 0.8826
P = 0.7784
Number of cells (*10⁴)
WT (Il33f/f)
KO (Gfapcrell33)
H
CNS CD4+ T cells
Number of CD4+ T cells
P =0.4654
Number of Foxp3+ T cells
P = 0.7870
Number of IL-17A+ T clles
P = 0.3873
Number of IFN-γ+ T cells
P = 0.5404
Number of GM-CSF+ T cells
P = 0.6012
WT (Il33f/f)
KO (Gfapcrell33)
I
Splenic CD4+ T cells
Number of CD4+ T cells
P = 0.1567
Number of Foxp3+ T cells
P = 0.2056
Number of IL-17A+ T cells
P = 0.1835
Number of IFN-γ+ T cells
P = 0.3170
Number of GM-CSF+ T cells
P = 0.2832
WT (Il33f/f)
KO (Gfapcrell33)
J
Isotype
WT (Il33f/f)
KO (GfapCrell33)
0.83%
11.6%
12.2%
FOXP3
AREG
% of Foxp3+Areg+ Treg
P = 0.4611
Number of Foxp3+Areg+ Treg
P = 0.6309
WT (Il33f/f)
KO (Gfapcrell33)
K
KO (Gfapcrell33)
WT (Il33f/f)
Isotype
Areg
Treg
Areg (MFI)
P =0.5309
WT (Il33f/f)
KO (Gfapcrell33)

Fig. S14: Control analyses of *Gfap::Cre;Il33(f/f)* EAE mice. (A) Analysis of *Il33* expression by qPCR in astrocytes or microglia isolated from EAE mice. n=5 per group. Unpaired two-tailed t-test. **(B)** Immunostaining of IL-33 in astrocytes demonstrating knockout in *Gfap::Cre;Il33(f/f)* mice. Representative image from N=3 mice. **(C)** Quantification of TMEM119+ cells in the spinal cord of naïve or EAE mice. n=6 images per group from N=3 mice. Unpaired two-tailed t-test. **(D)** Quantification of P2RY12+ AREG+ microglia in the spinal cord across EAE. n=6 images per group from N=3 mice. Unpaired two-tailed t-test. **(E)** Quantification of the number of AREG+ Iba1+ cells in naïve or EAE mice. n=6 images from N=3 mice per group. Unpaired two-tailed t-test. **(F)** Quantification of the number of P2RY12+ cells within TMEM119+ cells in the spinal cord. n=6 images per group from N=3 mice. Unpaired two-tailed t-test. **(G-I)** Quantification of astrocytes, microglia, and CNS-recruited monocytes (G) (n=7 per group) as well as CNS-recruited (H) and splenic (I) T cells (n=3-4 per group). Unpaired two-tailed t-test. **(J)** Quantification of the number of CNS-recruited AREG+ FoxP3+ Tregs from *Gfap::Cre;Il33(f/f)* mice or controls. n=5 per group. Unpaired two-tailed t-test. **(K)** Analysis of AREG expression by MFI in CNS-recruited Tregs from *Gfap::Cre;Il33(f/f)* mice or controls. n=5 per group. Unpaired two-tailed t-test.

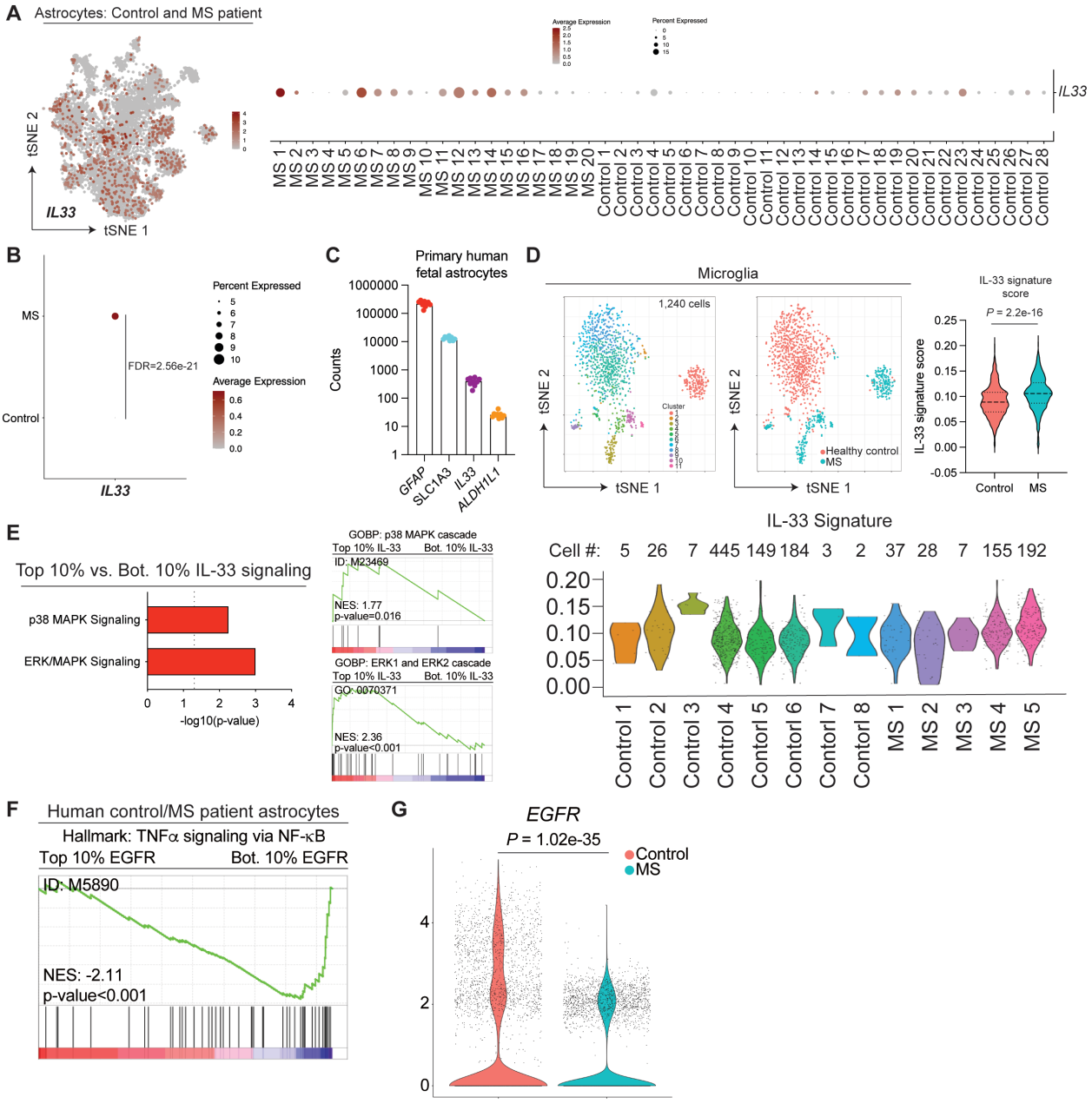
A
Astrocytes: Control and MS patient
tSNE 2
tSNE 1
IL33
Average Expression
Percent Expressed
IL33
MS 1 MS 2 MS 3 MS 4 MS 5 MS 6 MS 7 MS 8 MS 9 MS 10 MS 11 MS 12 MS 13 MS 14 MS 15 MS 16 MS 17 MS 18 MS 19 MS 20 Control 1 Control 2 Control 3 Control 4 Control 5 Control 6 Control 7 Control 8 Control 9 Control 10 Control 11 Control 12 Control 13 Control 14 Control 15 Control 16 Control 17 Control 18 Control 19 Control 20 Control 21 Control 22 Control 23 Control 24 Control 25 Control 26 Control 27 Control 28
B
MS
Control
FDR=2.56e-21
Percent Expressed
Average Expression
IL33
C
Primary human fetal astrocytes
Counts
GFAP
SLC1A3
IL33
ALDH1L1
D
Microglia
1,240 cells
Cluster
tSNE 2
tSNE 1
Healthy control
MS
IL-33 signature score
P = 2.2e-16
IL-33 signature score
Control
MS
E
Top 10% vs. Bot. 10% IL-33 signaling
p38 MAPK Signaling
ERK/MAPK Signaling
-log10(p-value)
GOBP: p38 MAPK cascade
Top 10% IL-33
Bot. 10% IL-33
ID: M23469
NES: 1.77
p-value=0.016
GOBP: ERK1 and ERK2 cascade
Top 10% IL-33
Bot. 10% IL-33
GO: 0070371
NES: 2.36
p-value<0.001
IL-33 Signature
Cell #: 5 26 7 445 149 184 3 2 37 28 7 155 192
Control 1 Control 2 Control 3 Control 4 Contorl 5 Contorl 6 Contorl 7 Contorl 8 MS 1 MS 2 MS 3 MS 4 MS 5
F
Human control/MS patient astrocytes
Hallmark: TNFα signaling via NF-κB
Top 10% EGFR
Bot. 10% EGFR
ID: M5890
NES: -2.11
p-value<0.001
G
EGFR
P = 1.02e-35
Control
MS

Fig. S15: IL-33-ST2 signaling is dysregulated in MS. (A) Feature plot of *IL33* in astrocytes isolated from MS patients or controls (n=48) previously reported in (*27*). **(B)** Quantification of IL33 expression in MS or controls by pseudobulk analysis. **(C)** Quantification of *IL33* expression in primary human fetal astrocytes by RNA-seq. n=9 per gene. **(D)** Analysis of an *IL33* signature in microglia analyzed from MS patients and controls previously studied in (*33*). **(E)** Validation of IL-33-driven pathways detected in MS patient and control microglia from (*33*) exhibiting the highest 10% versus lowest 10% IL-33 signaling, using a signature score for IL-33 previously reported in (*91*). **(F)** Negative association of EGFR signature score with NF-κB signaling analyzed in MS and control astrocytes previously studied in (*27*). **(G)** Quantification of EGFR expression in control or MS patient astrocytes from (A).

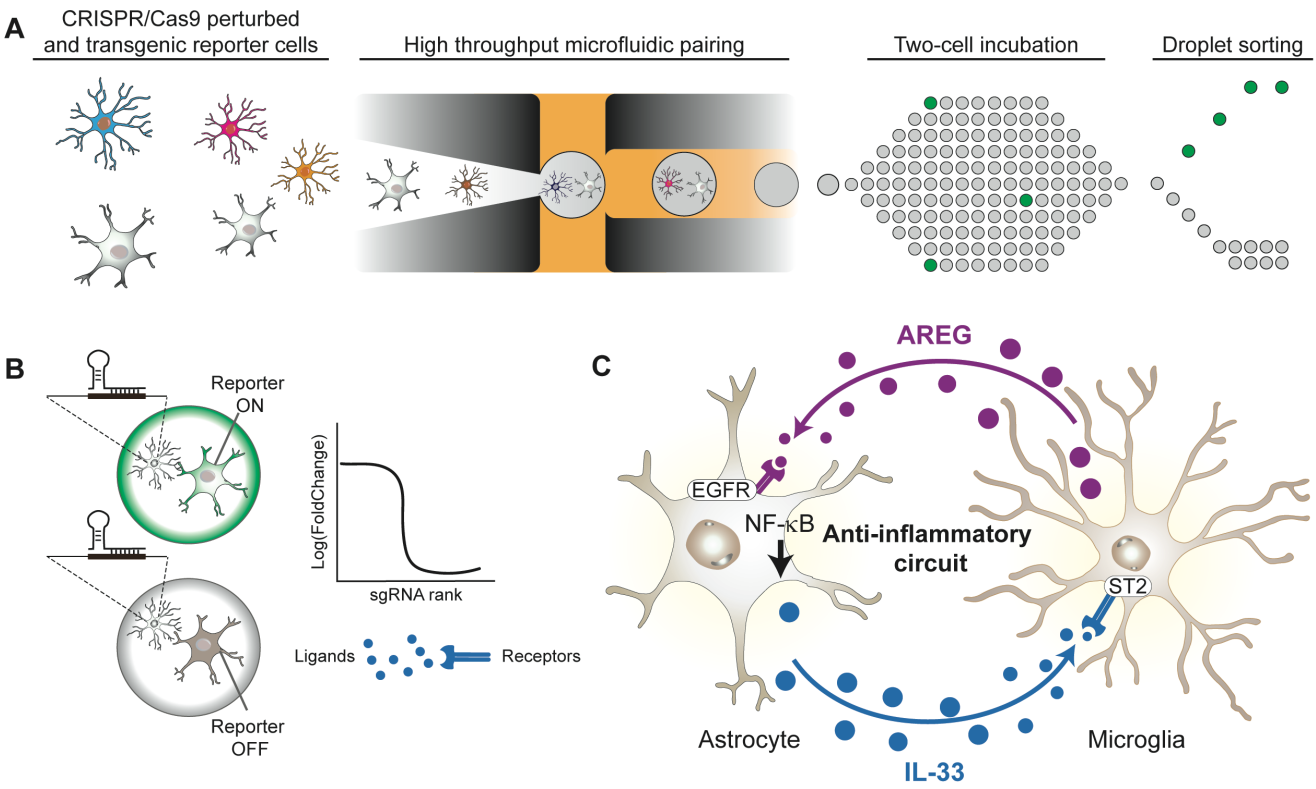
A
CRISPR/Cas9 perturbed
and transgenic reporter cells
High throughput microfluidic pairing
Two-cell incubation
Droplet sorting
B
Reporter
ON
Reporter
OFF
Log(FoldChange)
sgRNA rank
Ligands
Receptors
C
AREG
EGFR
NF-κB
Anti-inflammatory
circuit
ST2
Astrocyte
Microglia
IL-33

Fig. S16: Graphical abstract. (A) Schematic of SPEAC-seq platform for forward genetic screens of cell-cell interaction mechanisms in droplets. **(B)** Identification of genes that mediate astrocyte-microglia communication. **(C)** Proposed astrocyte-microglia regulatory circuit mediated by amphiregulin and IL33-ST2 signaling.

Movie S1: Sorting of cell pairs in droplets. Droplets containing varying numbers of cells flow from inlet (first channel from left) into sorting microfluidic chamber co-flowed with bias oil (second channel from left) where a central electrode triggers their entry into either a positive sort channel (third channel from left) or a waste channel (fourth channel from left). Note the entry of a two-cell containing droplet into the positive sort channel. Video speed is 5 frames/second.

Data S1 (separate file)

Differential gene expression analysis of primary mouse microglia in droplets treated with LPS versus vehicle-treated cells.

Data S2 (separate file)

Differential gene expression analysis of primary mouse microglia in adherent culture treated with LPS versus vehicle-treated cells.

Data S3 (separate file)

SPEAC-seq hits filtered against gene expression determined by RNA-seq of primary mouse microglia. This experiment analyzed EGFP+ versus EGFP- droplets containing $p65^{EGFP}$ astrocytes pre-treated with a subthreshold dose of 10^{-7} TNFα/IL-1β that were co-encapsulated with microglia transduced with a genome-wide CRISPR/Cas9 library and stimulated for 24 hours with LPS.

Data S4 (separate file)

SPEAC-seq hits detected in the indicated perturbed cell co-encapsulated with $p65^{EGFP}$ astrocytes from the indicated screens in Fig. S6.

Data S5 (separate file)

Analysis of the average gene expression of the SPEAC-seq hits uncovered in microglia detected in the indicated previously published studies of bulk or single-cell RNA-seq data.

Data S6 (separate file)

Genes detected in the regulatory networks corresponding to the indicated Figure panels.

Data S7 (separate file)

Analysis by RNA-seq of primary mouse astrocytes treated with AREG +/- 10 ng/mL IL-1β/TNFα.

Data S8 (separate file)

Analysis by RNA-seq of primary mouse astrocytes cultured in droplets and co-encapsulated with AREG.

Data S9 (separate file)

Analysis by RNA-seq of primary mouse astrocytes in adherent cultured and treated with AREG.

Data S10 (separate file)

Analysis by RNA-seq of primary mouse astrocytes isolated by flow cytometry following intracranial injection of AREG into the CNS.

Data S11 (separate file)

Gene expression fold changes in astrocytes treated with 10 ng/mL AREG in plates versus astrocytes treated with 10 ng/mL AREG in droplets. Statistical values were generated by normalizing the average of each gene fold change versus the mean control value within conditions, and then testing for the difference between conditions by Wilcoxon signed-rank test.

Data S12 (separate file)

Differentially expressed genes in microglia isolated from *Itgam::sgAreg* EAE mice compared against *Itgam::sgScrmbl* EAE mice.

Data S13 (separate file)

Differentially expressed genes in TdTomato+ astrocytes isolated from *Itgam::sgAreg* EAE *Aldh1l1::CreERT2*;*TdTomato*(f/+) mice compared against *Itgam::sgScrmbl* EAE *Aldh1l1::CreERT2*;*TdTomato*(f/+) mice.

Data S14 (separate file)

Differentially expressed genes in astrocytes isolated from *Cx3cr1::CreERT2;Il1rl1(f/f)* EAE mice compared against *Il1rl1(f/f)* EAE mice.

Data S15 (separate file)

Differentially expressed genes in microglia isolated from *Cx3cr1::CreERT2;Il1rl1(f/f)* EAE mice compared against *Il1rl1(f/f)* EAE mice.

Data S16 (separate file)

Differentially expressed genes in microglia isolated from *Gfap::Cre;Il33(f/f)* EAE mice compared against *Il33(f/f)* EAE mice.

Data S17 (separate file)

List of pathways detected in human microglia from MS patients or controls exhibiting an IL-33 signature score in the top 10% or bottom 10%.

References and Notes

1. D. S. Reich, C. F. Lucchinetti, P. A. Calabresi, Multiple Sclerosis. *N. Engl. J. Med.* **378**, 169–180 (2018). doi:10.1056/NEJMra1401483 Medline

2. R. T. Han, R. D. Kim, A. V. Molofsky, S. A. Liddelow, Astrocyte-immune cell interactions in physiology and pathology. *Immunity* **54**, 211–224 (2021). doi:10.1016/j.immuni.2021.01.013 Medline

3. M. Linnerbauer, M. A. Wheeler, F. J. Quintana, Astrocyte Crosstalk in CNS Inflammation. *Neuron* **108**, 608–622 (2020). doi:10.1016/j.neuron.2020.08.012 Medline

4. M. Prinz, T. Masuda, M. A. Wheeler, F. J. Quintana, Microglia and Central Nervous System-Associated Macrophages-From Origin to Disease Modulation. *Annu. Rev. Immunol.* **39**, 251–277 (2021). doi:10.1146/annurev-immunol-093019-110159 Medline

5. L. M. Sanmarco, C. M. Polonio, M. A. Wheeler, F. J. Quintana, Functional immune cell-astrocyte interactions. *J. Exp. Med.* **218**, e20202715 (2021). doi:10.1084/jem.20202715 Medline

6. L. Schirmer, D. P. Schafer, T. Bartels, D. H. Rowitch, P. A. Calabresi, Diversity and Function of Glial Cell Types in Multiple Sclerosis. *Trends Immunol.* **42**, 228–247 (2021). doi:10.1016/j.it.2021.01.005 Medline

7. B. S. Khakh, B. Deneen, The Emerging Nature of Astrocyte Diversity. *Annu. Rev. Neurosci.* **42**, 187–207 (2019). doi:10.1146/annurev-neuro-070918-050443 Medline

8. X. Yu, B. S. Khakh, SnapShot: Astrocyte interactions. *Cell* **185**, 220–220.e1 (2022). doi:10.1016/j.cell.2021.09.029 Medline

9. S. A. Liddelow, K. A. Guttenplan, L. E. Clarke, F. C. Bennett, C. J. Bohlen, L. Schirmer, M. L. Bennett, A. E. Münch, W.-S. Chung, T. C. Peterson, D. K. Wilton, A. Frouin, B. A. Napier, N. Panicker, M. Kumar, M. S. Buckwalter, D. H. Rowitch, V. L. Dawson, T. M. Dawson, B. Stevens, B. A. Barres, Neurotoxic reactive astrocytes are induced by activated microglia. *Nature* **541**, 481–487 (2017). doi:10.1038/nature21029 Medline

10. I. D. Vainchtein, G. Chin, F. S. Cho, K. W. Kelley, J. G. Miller, E. C. Chien, S. A. Liddelow, P. T. Nguyen, H. Nakao-Inoue, L. C. Dorman, O. Akil, S. Joshita, B. A. Barres, J. T. Paz, A. B. Molofsky, A. V. Molofsky, Astrocyte-derived interleukin-33 promotes microglial synapse engulfment and neural circuit development. *Science* **359**, 1269–1273 (2018). doi:10.1126/science.aal3589 Medline

11. V. Rothhammer, D. M. Borucki, E. C. Tjon, M. C. Takenaka, C.-C. Chao, A. Ardura-Fabregat, K. A. de Lima, C. Gutiérrez-Vázquez, P. Hewson, O. Staszewski, M. Blain, L. Healy, T. Neziraj, M. Borio, M. Wheeler, L. L. Dragin, D. A. Laplaud, J. Antel, J. I. Alvarez, M. Prinz, F. J. Quintana, Microglial control of astrocytes in response to microbial metabolites. *Nature* **557**, 724–728 (2018). doi:10.1038/s41586-018-0119-x Medline

12. I. C. Clark, C. Gutiérrez-Vázquez, M. A. Wheeler, Z. Li, V. Rothhammer, M. Linnerbauer, L. M. Sanmarco, L. Guo, M. Blain, S. E. J. Zandee, C.-C. Chao, K. V. Batterman, M. Schwabenland, P. Lotfy, A. Tejeda-Velarde, P. Hewson, C. Manganeli Polonio, M. W. Shultis, Y. Salem, E. C. Tjon, P. H. Fonseca-Castro, D. M. Borucki, K. Alves de Lima, A. Plasencia, A. R. Abate, D. L. Rosene, K. J. Hodgetts, M. Prinz, J. P. Antel, A. Prat, F. J. Quintana, Barcoded viral tracing of single-cell interactions in central nervous system inflammation. *Science* **372**, eabf1230 (2021). doi:10.1126/science.abf1230 Medline

13. M. A. Wheeler, M. Jaronen, R. Covacu, S. E. J. Zandee, G. Scalisi, V. Rothhammer, E. C. Tjon, C.-C. Chao, J. E. Kenison, M. Blain, V. T. S. Rao, P. Hewson, A. Barroso, C.

Gutiérrez-Vázquez, A. Prat, J. P. Antel, R. Hauser, F. J. Quintana, Environmental Control of Astrocyte Pathogenic Activities in CNS Inflammation. *Cell* **176**, 581–596.e18 (2019). doi:10.1016/j.cell.2018.12.012 Medline

14. A. Giladi, M. Cohen, C. Medaglia, Y. Baran, B. Li, M. Zada, P. Bost, R. Blecher-Gonen, T.-M. Salame, J. U. Mayer, E. David, F. Ronchese, A. Tanay, I. Amit, Dissecting cellular crosstalk by sequencing physically interacting cells. *Nat. Biotechnol.* **38**, 629–637 (2020). doi:10.1038/s41587-020-0442-2 Medline

15. R. Vento-Tormo, M. Efremova, R. A. Botting, M. Y. Turco, M. Vento-Tormo, K. B. Meyer, J.-E. Park, E. Stephenson, K. Polański, A. Goncalves, L. Gardner, S. Holmqvist, J. Henriksson, A. Zou, A. M. Sharkey, B. Millar, B. Innes, L. Wood, A. Wilbrey-Clark, R. P. Payne, M. A. Ivarsson, S. Lisgo, A. Filby, D. H. Rowitch, J. N. Bulmer, G. J. Wright, M. J. T. Stubbington, M. Haniffa, A. Moffett, S. A. Teichmann, Single-cell reconstruction of the early maternal-fetal interface in humans. *Nature* **563**, 347–353 (2018). doi:10.1038/s41586-018-0698-6 Medline

16. G. Pasqual, A. Chudnovskiy, J. M. J. Tas, M. Agudelo, L. D. Schweitzer, A. Cui, N. Hacohen, G. D. Victora, Monitoring T cell-dendritic cell interactions in vivo by intercellular enzymatic labelling. *Nature* **553**, 496–500 (2018). doi:10.1038/nature25442 Medline

17. S. Chen, N. E. Sanjana, K. Zheng, O. Shalem, K. Lee, X. Shi, D. A. Scott, J. Song, J. Q. Pan, R. Weissleder, H. Lee, F. Zhang, P. A. Sharp, Genome-wide CRISPR screen in a mouse model of tumor growth and metastasis. *Cell* **160**, 1246–1260 (2015). doi:10.1016/j.cell.2015.02.038 Medline

18. R. D. Chow, G. Wang, L. Ye, A. Codina, H. R. Kim, L. Shen, M. B. Dong, Y. Errami, S. Chen, In vivo profiling of metastatic double knockouts through CRISPR-Cpf1 screens. *Nat. Methods* **16**, 405–408 (2019). doi:10.1038/s41592-019-0371-5 Medline

19. M. W. LaFleur, T. H. Nguyen, M. A. Coxe, K. B. Yates, J. D. Trombley, S. A. Weiss, F. D. Brown, J. E. Gillis, D. J. Coxe, J. G. Doench, W. N. Haining, A. H. Sharpe, A CRISPR-Cas9 delivery system for in vivo screening of genes in the immune system. *Nat. Commun.* **10**, 1668 (2019). doi:10.1038/s41467-019-09656-2 Medline

20. R. T. Manguso, H. W. Pope, M. D. Zimmer, F. D. Brown, K. B. Yates, B. C. Miller, N. B. Collins, K. Bi, M. W. LaFleur, V. R. Juneja, S. A. Weiss, J. Lo, D. E. Fisher, D. Miao, E. Van Allen, D. E. Root, A. H. Sharpe, J. G. Doench, W. N. Haining, In vivo CRISPR screening identifies Ptpn2 as a cancer immunotherapy target. *Nature* **547**, 413–418 (2017). doi:10.1038/nature23270 Medline

21. D. Pan, A. Kobayashi, P. Jiang, L. Ferrari de Andrade, R. E. Tay, A. M. Luoma, D. Tsoucas, X. Qiu, K. Lim, P. Rao, H. W. Long, G.-C. Yuan, J. Doench, M. Brown, X. S. Liu, K. W. Wucherpfennig, A major chromatin regulator determines resistance of tumor cells to T cell-mediated killing. *Science* **359**, 770–775 (2018). doi:10.1126/science.aao1710 Medline

22. K. W. Wucherpfennig, A. N. Cartwright, Genetic screens to study the immune system in cancer. *Curr. Opin. Immunol.* **41**, 55–61 (2016). doi:10.1016/j.coi.2016.05.007 Medline

23. H. Yin, W. Xue, D. G. Anderson, CRISPR-Cas: A tool for cancer research and therapeutics. *Nat. Rev. Clin. Oncol.* **16**, 281–295 (2019). doi:10.1038/s41571-019-0166-8 Medline

24. A. Dixit, O. Parnas, B. Li, J. Chen, C. P. Fulco, L. Jerby-Arnon, N. D. Marjanovic, D. Dionne, T. Burks, R. Raychowdhury, B. Adamson, T. M. Norman, E. S. Lander, J. S. Weissman, N. Friedman, A. Regev, Perturb-Seq: Dissecting Molecular Circuits with Scalable Single-Cell

RNA Profiling of Pooled Genetic Screens. *Cell* **167**, 1853–1866.e17 (2016). doi:10.1016/j.cell.2016.11.038 Medline

25. I. C. Clark, R. Thakur, A. R. Abate, Concentric electrodes improve microfluidic droplet sorting. *Lab Chip* **18**, 710–713 (2018). doi:10.1039/C7LC01242J Medline

26. M. B. Everhart, W. Han, T. P. Sherrill, M. Arutiunov, V. V. Polosukhin, J. R. Burke, R. T. Sadikot, J. W. Christman, F. E. Yull, T. S. Blackwell, Duration and intensity of NF-κB activity determine the severity of endotoxin-induced acute lung injury. *J. Immunol.* **176**, 4995–5005 (2006). doi:10.4049/jimmunol.176.8.4995 Medline

27. M. A. Wheeler, I. C. Clark, E. C. Tjon, Z. Li, S. E. J. Zandee, C. P. Couturier, B. R. Watson, G. Scalisi, S. Alkwai, V. Rothhammer, A. Rotem, J. A. Heyman, S. Thaploo, L. M. Sanmarco, J. Ragoussis, D. A. Weitz, K. Petrecca, J. R. Moffitt, B. Becher, J. P. Antel, A. Prat, F. J. Quintana, MAFG-driven astrocytes promote CNS inflammation. *Nature* **578**, 593–599 (2020). doi:10.1038/s41586-020-1999-0 Medline

28. M. V. Sofroniew, Astrocyte barriers to neurotoxic inflammation. *Nat. Rev. Neurosci.* **16**, 249–263 (2015). doi:10.1038/nrn3898 Medline

29. J. G. Doench, N. Fusi, M. Sullender, M. Hegde, E. W. Vaimberg, K. F. Donovan, I. Smith, Z. Tothova, C. Wilen, R. Orchard, H. W. Virgin, J. Listgarten, D. E. Root, Optimized sgRNA design to maximize activity and minimize off-target effects of CRISPR-Cas9. *Nat. Biotechnol.* **34**, 184–191 (2016). doi:10.1038/nbt.3437 Medline

30. V. Rothhammer, I. D. Mascanfroni, L. Bunse, M. C. Takenaka, J. E. Kenison, L. Mayo, C.-C. Chao, B. Patel, R. Yan, M. Blain, J. I. Alvarez, H. Kébir, N. Anandasabapathy, G. Izquierdo, S. Jung, N. Obholzer, N. Pochet, C. B. Clish, M. Prinz, A. Prat, J. Antel, F. J. Quintana, Type I interferons and microbial metabolites of tryptophan modulate astrocyte activity and central nervous system inflammation via the aryl hydrocarbon receptor. *Nat. Med.* **22**, 586–597 (2016). doi:10.1038/nm.4106 Medline

31. C. K. Glass, K. Saijo, Nuclear receptor transrepression pathways that regulate inflammation in macrophages and T cells. *Nat. Rev. Immunol.* **10**, 365–376 (2010). doi:10.1038/nri2748 Medline

32. I. C. Clark, M. A. Wheeler, H.-G. Lee, Z. Li, L. M. Sanmarco, S. Thaploo, C. M. Polonio, S. W. Shin, G. Scalisi, A. R. Henry, J. M. Rone, F. Giovannoni, M. Charabati, C. F. Akl, D. M. Aleman, S. E. J. Zandee, A. Prat, D. C. Douek, E. A. Boritz, F. J. Quintana, A. R. Abate, Identification of astrocyte regulators by nucleic acid cytometry. *Nature* **614**, 326–333 (2023). doi:10.1038/s41586-022-05613-0 Medline

33. T. Masuda, R. Sankowski, O. Staszewski, C. Böttcher, L. Amann, C. Sagar, C. Scheiwe, S. Nessler, P. Kunz, G. van Loo, V. A. Coenen, P. C. Reinacher, A. Michel, U. Sure, R. Gold, D. Grün, J. Priller, C. Stadelmann, M. Prinz, Spatial and temporal heterogeneity of mouse and human microglia at single-cell resolution. *Nature* **566**, 388–392 (2019). doi:10.1038/s41586-019-0924-x Medline

34. Y. Zhou, W. M. Song, P. S. Andhey, A. Swain, T. Levy, K. R. Miller, P. L. Poliani, M. Cominelli, S. Grover, S. Gilfillan, M. Cella, T. K. Ulland, K. Zaitsev, A. Miyashita, T. Ikeuchi, M. Sainouchi, A. Kakita, D. A. Bennett, J. A. Schneider, M. R. Nichols, S. A. Beausoleil, J. D. Ulrich, D. M. Holtzman, M. N. Artyomov, M. Colonna, Human and mouse single-nucleus transcriptomics reveal TREM2-dependent and TREM2-independent cellular responses in Alzheimer's disease. *Nat. Med.* **26**, 131–142 (2020). doi:10.1038/s41591-019-0695-9 Medline

35. T. R. Hammond, C. Dufort, L. Dissing-Olesen, S. Giera, A. Young, A. Wysoker, A. J. Walker, F. Gergits, M. Segel, J. Nemesh, S. E. Marsh, A. Saunders, E. Macosko, F. Ginhoux, J. Chen, R. J. M. Franklin, X. Piao, S. A. McCarroll, B. Stevens, Single-Cell RNA Sequencing of Microglia throughout the Mouse Lifespan and in the Injured Brain Reveals Complex Cell-State Changes. *Immunity* **50**, 253–271.e6 (2019). doi:10.1016/j.immuni.2018.11.004 Medline

36. X. Jin, S. K. Simmons, A. Guo, A. S. Shetty, M. Ko, L. Nguyen, V. Jokhi, E. Robinson, P. Oyler, N. Curry, G. Deangeli, S. Lodato, J. Z. Levin, A. Regev, F. Zhang, P. Arlotta, In vivo Perturb-Seq reveals neuronal and glial abnormalities associated with autism risk genes. *Science* **370**, eaaz6063 (2020). doi:10.1126/science.aaz6063 Medline

37. L. M. Sanmarco, M. A. Wheeler, C. Gutiérrez-Vázquez, C. M. Polonio, M. Linnerbauer, F. A. Pinho-Ribeiro, Z. Li, F. Giovannoni, K. V. Batterman, G. Scalisi, S. E. J. Zandee, E. S. Heck, M. Alsuwailm, D. L. Rosene, B. Becher, I. M. Chiu, A. Prat, F. J. Quintana, Gut-licensed IFNγ^{+} NK cells drive LAMP1^{+}TRAIL^{+} anti-inflammatory astrocytes. *Nature* **590**, 473–479 (2021). doi:10.1038/s41586-020-03116-4 Medline

38. L. A. Monticelli, L. C. Osborne, M. Noti, S. V. Tran, D. M. W. Zaiss, D. Artis, IL-33 promotes an innate immune pathway of intestinal tissue protection dependent on amphiregulin-EGFR interactions. *Proc. Natl. Acad. Sci. U.S.A.* **112**, 10762–10767 (2015). doi:10.1073/pnas.1509070112 Medline

39. D. M. W. Zaiss, W. C. Gause, L. C. Osborne, D. Artis, Emerging functions of amphiregulin in orchestrating immunity, inflammation, and tissue repair. *Immunity* **42**, 216–226 (2015). doi:10.1016/j.immuni.2015.01.020 Medline

40. S. Krishnan, I. E. Prise, K. Wemyss, L. P. Schenck, H. M. Bridgeman, F. A. McClure, T. Zangerle-Murray, C. O'Boyle, T. A. Barbera, F. Mahmood, D. M. E. Bowdish, D. M. W. Zaiss, J. R. Grainger, J. E. Konkel, Amphiregulin-producing γδ T cells are vital for safeguarding oral barrier immune homeostasis. *Proc. Natl. Acad. Sci. U.S.A.* **115**, 10738–10743 (2018). doi:10.1073/pnas.1802320115 Medline

41. C. M. Minutti, R. V. Modak, F. Macdonald, F. Li, D. J. Smyth, D. A. Dorward, N. Blair, C. Husovsky, A. Muir, E. Giampazolias, R. Dobie, R. M. Maizels, T. J. Kendall, D. W. Griggs, M. Kopf, N. C. Henderson, D. M. Zaiss, A Macrophage-Pericyte Axis Directs Tissue Restoration via Amphiregulin-Induced Transforming Growth Factor Beta Activation. *Immunity* **50**, 645–654.e6 (2019). doi:10.1016/j.immuni.2019.01.008 Medline

42. A. M. Tsou, H. Yano, C. N. Parkhurst, T. Mahlakõiv, C. Chu, W. Zhang, Z. He, K. J. Jarick, C. Zhong, G. G. Putzel, M. Hatazaki, I. C. Lorenz, D. Andrew, P. Balderes, C. S. N. Klose, S. A. Lira, D. Artis, T. Ciecierega, A. Solomon, E. Barfield, K. Chien, J. Ferreira, J. Williams, S. Khan, P. S. Chong, S. Mozumder, L. Chou, W. Zhou, A. Ahmed, A. M. Joseph, I. C. Lorenz, D. Andrew, P. Balderes, C. S. N. Klose, S. A. Lira, D. Artis; JRI IBD Live Cell Bank Consortium, Neuropeptide regulation of non-redundant ILC2 responses at barrier surfaces. *Nature* **611**, 787–793 (2022). doi:10.1038/s41586-022-05297-6 Medline

43. M. Ito, K. Komai, S. Mise-Omata, M. Iizuka-Koga, Y. Noguchi, T. Kondo, R. Sakai, K. Matsuo, T. Nakayama, O. Yoshie, H. Nakatsukasa, S. Chikuma, T. Shichita, A. Yoshimura, Brain regulatory T cells suppress astrogliosis and potentiate neurological recovery. *Nature* **565**, 246–250 (2019). doi:10.1038/s41586-018-0824-5 Medline

44. J. Pohar, R. O'Connor, B. Manfroi, M. El-Behi, L. Jouneau, P. Boudinot, M. Bunse, W. Uckert, M. Luka, M. Ménager, R. Liblau, S. M. Anderton, S. Fillatreau, Antigen receptor-engineered Tregs inhibit CNS autoimmunity in cell therapy using nonredundant immune

mechanisms in mice. *Eur. J. Immunol.* **52**, 1335–1349 (2022). doi:10.1002/eji.202249845 Medline

45. H. R. Jiang, M. Milovanović, D. Allan, W. Niedbala, A.-G. Besnard, S. Y. Fukada, J. C. Alves-Filho, D. Togbe, C. S. Goodyear, C. Linington, D. Xu, M. L. Lukic, F. Y. Liew, IL-33 attenuates EAE by suppressing IL-17 and IFN-γ production and inducing alternatively activated macrophages. *Eur. J. Immunol.* **42**, 1804–1814 (2012). doi:10.1002/eji.201141947 Medline

46. D. Yang, Z. Han, J. J. Oppenheim, Alarmins and immunity. *Immunol. Rev.* **280**, 41–56 (2017). doi:10.1111/imr.12577 Medline

47. S. P. Gadani, J. T. Walsh, I. Smirnov, J. Zheng, J. Kipnis, The glia-derived alarmin IL-33 orchestrates the immune response and promotes recovery following CNS injury. *Neuron* **85**, 703–709 (2015). doi:10.1016/j.neuron.2015.01.013 Medline

48. D. He, H. Xu, H. Zhang, R. Tang, Y. Lan, R. Xing, S. Li, E. Christian, Y. Hou, P. Lorello, B. Caldarone, J. Ding, L. Nguyen, D. Dionne, P. Thakore, A. Schnell, J. R. Huh, O. Rozenblatt-Rosen, A. Regev, V. K. Kuchroo, Disruption of the IL-33-ST2-AKT signaling axis impairs neurodevelopment by inhibiting microglial metabolic adaptation and phagocytic function. *Immunity* **55**, 159–173.e9 (2022). doi:10.1016/j.immuni.2021.12.001 Medline

49. M. Funakoshi-Tago, K. Tago, M. Hayakawa, S. Tominaga, T. Ohshio, Y. Sonoda, T. Kasahara, TRAF6 is a critical signal transducer in IL-33 signaling pathway. *Cell. Signal.* **20**, 1679–1686 (2008). doi:10.1016/j.cellsig.2008.05.013 Medline

50. B. Demaree, C. L. Delley, H. N. Vasudevan, C. A. C. Peretz, D. Ruff, C. C. Smith, A. R. Abate, Joint profiling of DNA and proteins in single cells to dissect genotype-phenotype associations in leukemia. *Nat. Commun.* **12**, 1583 (2021). doi:10.1038/s41467-021-21810-3 Medline

51. A. M. Klein, L. Mazutis, I. Akartuna, N. Tallapragada, A. Veres, V. Li, L. Peshkin, D. A. Weitz, M. W. Kirschner, Droplet barcoding for single-cell transcriptomics applied to embryonic stem cells. *Cell* **161**, 1187–1201 (2015). doi:10.1016/j.cell.2015.04.044 Medline

52. E. Z. Macosko, A. Basu, R. Satija, J. Nemesh, K. Shekhar, M. Goldman, I. Tirosh, A. R. Bialas, N. Kamitaki, E. M. Martersteck, J. J. Trombetta, D. A. Weitz, J. R. Sanes, A. K. Shalek, A. Regev, S. A. McCarroll, Highly Parallel Genome-wide Expression Profiling of Individual Cells Using Nanoliter Droplets. *Cell* **161**, 1202–1214 (2015). doi:10.1016/j.cell.2015.05.002 Medline

53. M. Stoeckius, C. Hafemeister, W. Stephenson, B. Houck-Loomis, P. K. Chattopadhyay, H. Swerdlow, R. Satija, P. Smibert, Simultaneous epitope and transcriptome measurement in single cells. *Nat. Methods* **14**, 865–868 (2017). doi:10.1038/nmeth.4380 Medline

54. R. A. Goodnow Jr., C. E. Dumelin, A. D. Keefe, DNA-encoded chemistry: Enabling the deeper sampling of chemical space. *Nat. Rev. Drug Discov.* **16**, 131–147 (2017). doi:10.1038/nrd.2016.213 Medline

55. W. G. Cochrane, M. L. Malone, V. Q. Dang, V. Cavett, A. L. Satz, B. M. Paegel, Activity-Based DNA-Encoded Library Screening. *ACS Comb. Sci.* **21**, 425–435 (2019). doi:10.1021/acscombsci.9b00037 Medline

56. D. Y. Kwon, Y. T. Zhao, J. M. Lamonica, Z. Zhou, Locus-specific histone deacetylation using a synthetic CRISPR-Cas9-based HDAC. *Nat. Commun.* **8**, 15315 (2017). doi:10.1038/ncomms15315 Medline

57. S. Konermann, M. D. Brigham, A. E. Trevino, J. Joung, O. O. Abudayyeh, C. Barcena, P. D. Hsu, N. Habib, J. S. Gootenberg, H. Nishimasu, O. Nureki, F. Zhang, Genome-scale transcriptional activation by an engineered CRISPR-Cas9 complex. *Nature* **517**, 583–588 (2015). doi:10.1038/nature14136 Medline

58. N. C. Yeo, A. Chavez, A. Lance-Byrne, Y. Chan, D. Menn, D. Milanova, C.-C. Kuo, X. Guo, S. Sharma, A. Tung, R. J. Cecchi, M. Tuttle, S. Pradhan, E. T. Lim, N. Davidsohn, M. R. Ebrahimkhani, J. J. Collins, N. E. Lewis, S. Kiani, G. M. Church, An enhanced CRISPR repressor for targeted mammalian gene regulation. *Nat. Methods* **15**, 611–616 (2018). doi:10.1038/s41592-018-0048-5 Medline

59. O. O. Abudayyeh, J. S. Gootenberg, P. Essletzbichler, S. Han, J. Joung, J. J. Belanto, V. Verdine, D. B. T. Cox, M. J. Kellner, A. Regev, E. S. Lander, D. F. Voytas, A. Y. Ting, F. Zhang, RNA targeting with CRISPR-Cas13. *Nature* **550**, 280–284 (2017). doi:10.1038/nature24049 Medline

60. K. A. Guttenplan, B. K. Stafford, R. N. El-Danaf, D. I. Adler, A. E. Münch, M. K. Weigel, A. D. Huberman, S. A. Liddelow, Neurotoxic Reactive Astrocytes Drive Neuronal Death after Retinal Injury. *Cell Rep.* **31**, 107776 (2020). doi:10.1016/j.celrep.2020.107776 Medline

61. C. Schiering, T. Krausgruber, A. Chomka, A. Fröhlich, K. Adelmann, E. A. Wohlfert, J. Pott, T. Griseri, J. Bollrath, A. N. Hegazy, O. J. Harrison, B. M. J. Owens, M. Löhning, Y. Belkaid, P. G. Fallon, F. Powrie, The alarmin IL-33 promotes regulatory T-cell function in the intestine. *Nature* **513**, 564–568 (2014). doi:10.1038/nature13577 Medline

62. N. Arpaia, J. A. Green, B. Moltedo, A. Arvey, S. Hemmers, S. Yuan, P. M. Treuting, A. Y. Rudensky, A Distinct Function of Regulatory T Cells in Tissue Protection. *Cell* **162**, 1078–1089 (2015). doi:10.1016/j.cell.2015.08.021 Medline

63. D. Burzyn, W. Kuswanto, D. Kolodin, J. L. Shadrach, M. Cerletti, Y. Jang, E. Sefik, T. G. Tan, A. J. Wagers, C. Benoist, D. Mathis, A special population of regulatory T cells potentiates muscle repair. *Cell* **155**, 1282–1295 (2013). doi:10.1016/j.cell.2013.10.054 Medline

64. H. G. Lee, M. A. Wheeler, F. J. Quintana, Function and therapeutic value of astrocytes in neurological diseases. *Nat. Rev. Drug Discov.* **21**, 339–358 (2022). doi:10.1038/s41573-022-00390-x Medline

65. B. Stevens, N. J. Allen, L. E. Vazquez, G. R. Howell, K. S. Christopherson, N. Nouri, K. D. Micheva, A. K. Mehalow, A. D. Huberman, B. Stafford, A. Sher, A. M. Litke, J. D. Lambris, S. J. Smith, S. W. M. John, B. A. Barres, The classical complement cascade mediates CNS synapse elimination. *Cell* **131**, 1164–1178 (2007). doi:10.1016/j.cell.2007.10.036 Medline

66. M. K. Pandey, T. A. Burrow, R. Rani, L. J. Martin, D. Witte, K. D. Setchell, M. A. Mckay, A. F. Magnusen, W. Zhang, B. Liou, J. Köhl, G. A. Grabowski, Complement drives glucosylceramide accumulation and tissue inflammation in Gaucher disease. *Nature* **543**, 108–112 (2017). doi:10.1038/nature21368 Medline

67. A. Sekar, A. R. Bialas, H. de Rivera, A. Davis, T. R. Hammond, N. Kamitaki, K. Tooley, J. Presumey, M. Baum, V. Van Doren, G. Genovese, S. A. Rose, R. E. Handsaker, M. J. Daly, M. C. Carroll, B. Stevens, S. A. McCarroll; Schizophrenia Working Group of the

Psychiatric Genomics Consortium, Schizophrenia risk from complex variation of complement component 4. *Nature* **530**, 177–183 (2016). doi:10.1038/nature16549 Medline

68. S. Sawada, J. D. Scarborough, N. Killeen, D. R. Littman, A lineage-specific transcriptional silencer regulates CD4 gene expression during T lymphocyte development. *Cell* **77**, 917–929 (1994). doi:10.1016/0092-8674(94)90140-6 Medline

69. R. Srinivasan, T.-Y. Lu, H. Chai, J. Xu, B. S. Huang, P. Golshani, G. Coppola, B. S. Khakh, New Transgenic Mouse Lines for Selectively Targeting Astrocytes and Studying Calcium Signals in Astrocyte Processes In Situ and In Vivo. *Neuron* **92**, 1181–1195 (2016). doi:10.1016/j.neuron.2016.11.030 Medline

70. L. Madisen, T. A. Zwingman, S. M. Sunkin, S. W. Oh, H. A. Zariwala, H. Gu, L. L. Ng, R. D. Palmiter, M. J. Hawrylycz, A. R. Jones, E. S. Lein, H. Zeng, A robust and high-throughput Cre reporting and characterization system for the whole mouse brain. *Nat. Neurosci.* **13**, 133–140 (2010). doi:10.1038/nn.2467 Medline

71. A. D. Garcia, N. B. Doan, T. Imura, T. G. Bush, M. V. Sofroniew, GFAP-expressing progenitors are the principal source of constitutive neurogenesis in adult mouse forebrain. *Nat. Neurosci.* **7**, 1233–1241 (2004). doi:10.1038/nn1340 Medline

72. W. Y. Chen, J. Hong, J. Gannon, R. Kakkar, R. T. Lee, Myocardial pressure overload induces systemic inflammation through endothelial cell IL-33. *Proc. Natl. Acad. Sci. U.S.A.* **112**, 7249–7254 (2015). doi:10.1073/pnas.1424236112 Medline

73. S. Yona, K.-W. Kim, Y. Wolf, A. Mildner, D. Varol, M. Breker, D. Strauss-Ayali, S. Viukov, M. Guilliams, A. Misharin, D. A. Hume, H. Perlman, B. Malissen, E. Zelzer, S. Jung, Fate mapping reveals origins and dynamics of monocytes and tissue macrophages under homeostasis. *Immunity* **38**, 79–91 (2013). doi:10.1016/j.immuni.2012.12.001 Medline

74. C. Gutiérrez-Vázquez, F. J. Quintana, Protocol for *in vitro* analysis of pro-inflammatory and metabolic functions of cultured primary murine astrocytes. *STAR Protoc.* **3**, 101033 (2021). doi:10.1016/j.xpro.2021.101033 Medline

75. J. Joung, S. Konermann, J. S. Gootenberg, O. O. Abudayyeh, R. J. Platt, M. D. Brigham, N. E. Sanjana, F. Zhang, Genome-scale CRISPR-Cas9 knockout and transcriptional activation screening. *Nat. Protoc.* **12**, 828–863 (2017). doi:10.1038/nprot.2017.016 Medline

76. S. A. Stewart, D. M. Dykxhoorn, D. Palliser, H. Mizuno, E. Y. Yu, D. S. An, D. M. Sabatini, I. S. Chen, W. C. Hahn, P. A. Sharp, R. A. Weinberg, C. D. Novina, Lentivirus-delivered stable gene silencing by RNAi in primary cells. *RNA* **9**, 493–501 (2003). doi:10.1261/rna.2192803 Medline

77. W. Li, H. Xu, T. Xiao, L. Cong, M. I. Love, F. Zhang, R. A. Irizarry, J. S. Liu, M. Brown, X. S. Liu, MAGeCK enables robust identification of essential genes from genome-scale CRISPR/Cas9 knockout screens. *Genome Biol.* **15**, 554 (2014). doi:10.1186/s13059-014-0554-4 Medline

78. K. A. Guttenplan, M. K. Weigel, D. I. Adler, J. Couthouis, S. A. Liddelow, A. D. Gitler, B. A. Barres, Knockout of reactive astrocyte activating factors slows disease progression in an ALS mouse model. *Nat. Commun.* **11**, 3753 (2020). doi:10.1038/s41467-020-17514-9 Medline

79. N. E. Sanjana, O. Shalem, F. Zhang, Improved vectors and genome-wide libraries for CRISPR screening. *Nat. Methods* **11**, 783–784 (2014). doi:10.1038/nmeth.3047 Medline

80. T. Wang, H. Yu, N. W. Hughes, B. Liu, A. Kendirli, K. Klein, W. W. Chen, E. S. Lander, D. M. Sabatini, Gene Essentiality Profiling Reveals Gene Networks and Synthetic Lethal Interactions with Oncogenic Ras. *Cell* **168**, 890–903.e15 (2017). doi:10.1016/j.cell.2017.01.013 Medline

81. C. C. Chao, C. Gutiérrez-Vázquez, V. Rothhammer, L. Mayo, M. A. Wheeler, E. C. Tjon, S. E. J. Zandee, M. Blain, K. A. de Lima, M. C. Takenaka, J. Avila-Pacheco, P. Hewson, L. Liu, L. M. Sanmarco, D. M. Borucki, G. Z. Lipof, S. A. Trauger, C. B. Clish, J. P. Antel, A. Prat, F. J. Quintana, Metabolic Control of Astrocyte Pathogenic Activity via cPLA2-MAVS. *Cell* **179**, 1483–1498.e22 (2019). doi:10.1016/j.cell.2019.11.016 Medline

82. L. C. Foo, Purification of rat and mouse astrocytes by immunopanning. *Cold Spring Harb. Protoc.* **2013**, 421–432 (2013). doi:10.1101/pdb.err080101 Medline

83. A. J. Thompson, B. L. Banwell, F. Barkhof, W. M. Carroll, T. Coetzee, G. Comi, J. Correale, F. Fazekas, M. Filippi, M. S. Freedman, K. Fujihara, S. L. Galetta, H. P. Hartung, L. Kappos, F. D. Lublin, R. A. Marrie, A. E. Miller, D. H. Miller, X. Montalban, E. M. Mowry, P. S. Sorensen, M. Tintoré, A. L. Traboulsee, M. Trojano, B. M. J. Uitdehaag, S. Vukusic, E. Waubant, B. G. Weinshenker, S. C. Reingold, J. A. Cohen, Diagnosis of multiple sclerosis: 2017 revisions of the McDonald criteria. *Lancet Neurol.* **17**, 162–173 (2018). doi:10.1016/S1474-4422(17)30470-2 Medline

84. T. Dhaeze, L. Tremblay, C. Lachance, E. Peelen, S. Zandee, C. Grasmuck, L. Bourbonnière, S. Larouche, X. Ayrignac, R.-M. Rébillard, J. Poirier, B. Lahav, P. Duquette, M. Girard, R. Moumdjian, A. Bouthillier, C. Larochelle, A. Prat, CD70 defines a subset of proinflammatory and CNS-pathogenic T_H1/T_H17 lymphocytes and is overexpressed in multiple sclerosis. *Cell. Mol. Immunol.* **16**, 652–665 (2019). doi:10.1038/s41423-018-0198-5 Medline

85. B. Broux, S. Zandee, E. Gowing, M. Charabati, M.-A. Lécuyer, O. Tastet, L. Hachehouche, L. Bourbonnière, J.-P. Ouimet, F. Lemaitre, S. Larouche, R. Cayrol, A. Bouthillier, R. Moumdjian, B. Lahav, J. Poirier, P. Duquette, N. Arbour, E. Peelen, A. Prat, Interleukin-26, preferentially produced by T_H17 lymphocytes, regulates CNS barrier function. *Neurol. Neuroimmunol. Neuroinflamm.* **7**, e870 (2020). doi:10.1212/NXI.0000000000000870 Medline

86. J. J. Trombetta, D. Gennert, D. Lu, R. Satija, A. K. Shalek, A. Regev, Preparation of Single-Cell RNA-Seq Libraries for Next Generation Sequencing. *Curr. Protoc. Mol. Biol.* **107**, 4.22.1–4.22.17 (2014). doi:10.1002/0471142727.mb0422s107 Medline

87. G. X. Zheng, J. M. Terry, P. Belgrader, P. Ryvkin, Z. W. Bent, R. Wilson, S. B. Ziraldo, T. D. Wheeler, G. P. McDermott, J. Zhu, M. T. Gregory, J. Shuga, L. Montesclaros, J. G. Underwood, D. A. Masquelier, S. Y. Nishimura, M. Schnall-Levin, P. W. Wyatt, C. M. Hindson, R. Bharadwaj, A. Wong, K. D. Ness, L. W. Beppu, H. J. Deeg, C. McFarland, K. R. Loeb, W. J. Valente, N. G. Ericson, E. A. Stevens, J. P. Radich, T. S. Mikkelsen, B. J. Hindson, J. H. Bielas, Massively parallel digital transcriptional profiling of single cells. *Nat. Commun.* **8**, 14049 (2017). doi:10.1038/ncomms14049 Medline

88. S. L. Wolock, R. Lopez, A. M. Klein, Scrublet: Computational Identification of Cell Doublets in Single-Cell Transcriptomic Data. *Cell Syst.* **8**, 281–291.e9 (2019). doi:10.1016/j.cels.2018.11.005 Medline

89. C. Hafemeister, R. Satija, Normalization and variance stabilization of single-cell RNA-seq data using regularized negative binomial regression. *Genome Biol.* **20**, 296 (2019). doi:10.1186/s13059-019-1874-1 Medline

90. A. Butler, P. Hoffman, P. Smibert, E. Papalexi, R. Satija, Integrating single-cell transcriptomic data across different conditions, technologies, and species. *Nat. Biotechnol.* **36**, 411–420 (2018). doi:10.1038/nbt.4096 Medline

91. P. T. Nguyen, L. C. Dorman, S. Pan, I. D. Vainchtein, R. T. Han, H. Nakao-Inoue, S. E. Taloma, J. J. Barron, A. B. Molofsky, M. A. Kheirbek, A. V. Molofsky, Microglial Remodeling of the Extracellular Matrix Promotes Synapse Plasticity. *Cell* **182**, 388–403.e15 (2020). doi:10.1016/j.cell.2020.05.050 Medline

92. G. Finak, A. McDavid, M. Yajima, J. Deng, V. Gersuk, A. K. Shalek, C. K. Slichter, H. W. Miller, M. J. McElrath, M. Prlic, P. S. Linsley, R. Gottardo, MAST: A flexible statistical framework for assessing transcriptional changes and characterizing heterogeneity in single-cell RNA sequencing data. *Genome Biol.* **16**, 278 (2015). doi:10.1186/s13059-015-0844-5 Medline

93. A. Subramanian, P. Tamayo, V. K. Mootha, S. Mukherjee, B. L. Ebert, M. A. Gillette, A. Paulovich, S. L. Pomeroy, T. R. Golub, E. S. Lander, J. P. Mesirov, Gene set enrichment analysis: A knowledge-based approach for interpreting genome-wide expression profiles. *Proc. Natl. Acad. Sci. U.S.A.* **102**, 15545–15550 (2005). doi:10.1073/pnas.0506580102 Medline

94. J. G. Pérez-Silva, M. Araujo-Voces, V. Quesada, nVenn: Generalized, quasi-proportional Venn and Euler diagrams. *Bioinformatics* **34**, 2322–2324 (2018). doi:10.1093/bioinformatics/bty109 Medline